



**HAL**  
open science

# Adipocyte Glucocorticoid Receptor Deficiency Promotes Adipose Tissue Expandability and Improves the Metabolic Profile Under Corticosterone Exposure

Héloïse Dalle, Marie Garcia, Bénédicte Antoine, Vanessa Boehm, Thi Thu Huong Do, Marion Buyse, Tatiana Ledent, Antonin Lamaziere, Christophe Magnan, Catherine Postic, et al.

## ► To cite this version:

Héloïse Dalle, Marie Garcia, Bénédicte Antoine, Vanessa Boehm, Thi Thu Huong Do, et al.. Adipocyte Glucocorticoid Receptor Deficiency Promotes Adipose Tissue Expandability and Improves the Metabolic Profile Under Corticosterone Exposure. *Diabetes*, 2019, 68 (2), pp.305-317. 10.2337/db17-1577 . hal-02348048

**HAL Id: hal-02348048**

**<https://hal.science/hal-02348048>**

Submitted on 15 Nov 2022

**HAL** is a multi-disciplinary open access archive for the deposit and dissemination of scientific research documents, whether they are published or not. The documents may come from teaching and research institutions in France or abroad, or from public or private research centers.

L'archive ouverte pluridisciplinaire **HAL**, est destinée au dépôt et à la diffusion de documents scientifiques de niveau recherche, publiés ou non, émanant des établissements d'enseignement et de recherche français ou étrangers, des laboratoires publics ou privés.



25

26

27 **Author contributions:**

28 # These authors should be considered co-last authors.

29

30 \*To whom correspondence should be addressed. E-mail : [marthe.moldes@inserm.fr](mailto:marthe.moldes@inserm.fr)

31 Address : INSERM UMR\_S938, Centre de Recherche Saint-Antoine, 27 rue de Chaligny, 75012,

32 Paris, France

33 Phone : +33 (0)1 40 01 13 21

34 Fax : +33 (0)1 40 01 14 32

35

36 **ABSTRACT**

37 Widely used for their anti-inflammatory and immunosuppressive properties, glucocorticoids are  
38 nonetheless responsible for the development of diabetes and lipodystrophy. Despite an increasing  
39 number of studies focused on adipocyte glucocorticoid receptor (GR), its precise role in the  
40 molecular mechanisms of these complications remains unclear. In keeping with this goal, we  
41 generated a conditional adipocyte specific murine model of GR invalidation (AdipoGR-KO mice).  
42 Interestingly, when submitted to a corticosterone treatment to mimic hypercorticism conditions,  
43 AdipoGR-KO mice exhibited an improved glucose tolerance and insulin sensitivity. This was  
44 related to the adipose-specific activation of insulin signaling pathway, which contributed to fat  
45 mass expansion, as well as a shift towards an anti-inflammatory macrophage polarization in  
46 adipose tissue of AdipoGR-KO animals. Moreover, these mice were protected against ectopic lipid  
47 accumulation in liver and displayed an improved lipid profile, contributing to their overall healthier  
48 phenotype. Altogether, our results indicate that adipocyte GR is a key factor of adipose tissue  
49 expansion and glucose and lipid metabolism control, which should be taken into account in the  
50 further design of adipocyte GR selective modulators.

51

## 52 INTRODUCTION

53 Glucocorticoids (GCs) and synthetic analogues are among the most prescribed anti-inflammatory  
54 treatments (1). However high doses of GCs can lead to side effects including hyperglycemia,  
55 dyslipidemia, insulin resistance and lipodystrophy (2), which is characterized by an enlargement  
56 of visceral adipose tissue (VAT) at the expense of subcutaneous adipose tissue (SCAT). Conversely  
57 to the protective effect of SCAT expansion on metabolic disorders, VAT hypertrophy is a major  
58 risk factor for the development of diabetes and cardiovascular diseases (3). Thus, patients with  
59 endogenous hypercorticism (Cushing syndrome) harbor similar features with metabolic syndrome,  
60 suggesting a potential role of GCs in the pathophysiology of visceral obesity and insulin resistance  
61 (4).

62 GCs exert pleiotropic effects on adipose tissue (AT) physiology. They promote adipogenesis (5, 6)  
63 and regulate adipocyte lipid storage and mobilization, as well as adipokine secretion (5, 7, 8). These  
64 effects rely on the nature of subcutaneous or visceral AT, as well as on the GC concentration and  
65 duration of exposure (9-11). GC actions are mediated through two nuclear receptors, the  
66 glucocorticoid receptor (GR) and the mineralocorticoid receptor (MR) (7, 8), which play specific  
67 roles in the development and functions of adipocytes but also on AT pathophysiology (7, 8).

68 Global human MR overexpression in transgenic mice leads to resistance to high-fat diet-induced  
69 obesity by regulating adipocyte differentiation and macrophage polarization (12). However, this  
70 protective effect is abolished when MR is specifically overexpressed in AT leading to insulin  
71 resistance and metabolic syndrome under diet-induced obesity (13). Furthermore, *in vivo* MR  
72 pharmacological blockade by eplerenone reduces the expression of pro-inflammatory factors in  
73 genetically obese and diabetic mice, suggesting a role for MR as a key factor mediating obesity-  
74 related inflammation and insulin resistance (14). The implication of GR in the pathophysiology of  
75 metabolic syndrome has been suggested by the pharmacological blockade of GR (by RU486),

76 which improved fasting hyperinsulinemia, insulin resistance and glucose intolerance (15). More  
77 recently, the role of the adipocyte GR was investigated *in vivo* using constitutive murine models of  
78 adipocyte GR deletion (16-20). However, these studies led to contradictory results, where the  
79 adipocyte GR invalidation could either play a minor role in diet-induced obesity (17, 20) or have a  
80 metabolic impact protecting from age-related and diet-induced obesity (19). This metabolic  
81 improvement in adipocyte GR-deficient mice could involve the inhibition of negative feedback  
82 mechanisms in hypothalamic-pituitary-adrenal axis (16). Furthermore, studying the role of  
83 adipocyte GR in the context of GC-induced metabolic dysfunction also led to divergent results on  
84 insulin resistance improvement (18, 20). These discrepancies may rely on the murine model of  
85 constitutive GR invalidation that could profoundly modify the biology of adipose cells and tissue  
86 through compensatory mechanisms.

87 To circumvent the phenotypic impact of GR ablation on growth and developmental processes, we  
88 generated a mouse model of conditional GR invalidation specifically in AT of adult mice  
89 (AdipoGR-KO mice). To address the role of adipocyte GR implications under exogenous  
90 hypercorticism conditions, we submitted AdipoGR-KO mice to a 4-week corticosterone treatment.  
91 Interestingly, these mice exhibited an expansion in fat mass under corticosterone exposure. Despite  
92 increased adiposity, AdipoGR-KO mice displayed an improved metabolic profile, with a selective  
93 enhancement in AT insulin sensitivity. Furthermore, AdipoGR-KO mice harbored a normal plasma  
94 lipid profile and were protected from lipid ectopic deposition in liver. Thus, our results demonstrate  
95 that adipocyte GR is a key determinant of AT expandability and insulin sensitivity, which in turn  
96 influences whole body glucose and lipid homeostasis.

97

98

## 99 **Research design and methods**

### 100 **Animals and treatment**

101 Adipocyte-specific GR-deficient mice (AdipoGR-KO) were generated by crossing C57BL/6J  
102 GR<sup>Lox/Lox</sup> mice (kind gift of Dr Tronche, France (21)) with C57BL/6J mice, which express the  
103 CreERT2 recombinase under the adiponectin promoter (kind gift of Dr Offermanns, Germany  
104 (22)). Cre recombinase was activated by tamoxifene intraperitoneal injection in ten-week-old male  
105 mice (60 µg/g/day; MP Biomedicals, Illkirch Graffenstaden, France) for 5 consecutive days.  
106 Fourteen-week-old AdipoGR-KO and control (WT) mice were treated during 4 weeks either with  
107 corticosterone (CORT, 100 µg/ml; Sigma-Aldrich, St. Louis, MO) or vehicle (VEH, 1% ethanol)  
108 added to tap water as described in (23). Eighteen-week-old mice were then sacrificed. Tissues were  
109 dissected, rapidly frozen in liquid nitrogen and kept at -80°C. Blood was collected by intracardiac  
110 puncture with heparin-moistened syringes. Plasma was obtained after centrifugation at 5,000 x g  
111 for 10 min at 10°C.

112 The animal housing facility was granted approval (C 75-12-01) given by the French  
113 Administration. All experiments were conducted according to the European Communities Council  
114 Directive (2010/63/UE), and approved by the Regional Animal Care and use committee (Ile-de-  
115 France, Paris, no5; agreement number 00917.02 and 4625).

116

### 117 **Metabolic parameter exploration and *in vivo* insulin stimulation**

118 For Oral glucose tolerance tests (OGTTs), 5 hour-fasted mice received a glucose load (1 g/kg body  
119 weight) orally. For insulin tolerance tests (ITTs), mice fasted 5 hours were injected  
120 intraperitoneally with 1 UI/kg insulin (Actrapid Penfill; Novo Nordisk, Paris, France). Whole-tail  
121 vein blood was collected at baseline (T0) and 15 min (T15), centrifuged plasma samples were  
122 stored at -80°C. For both tests, blood glucose was measured at the tail vein using an automatic

123 Accu-Chek Performa glucometer (Roche, Meylan, France) at indicated times. For insulin-signaling  
124 experiments, mice were intraperitoneally injected with 1.5 UI /kg of human insulin (Actrapid  
125 Penfill; Novo Nordisk, Paris, France), sacrificed 10 min later and tissues were stored at -80°C.

126  
127 **Functional analyzes on adipose tissue explants**  
128 Functional analyzes were carried out on subcutaneous (SCAT) and gonadal adipose tissue (GAT)  
129 explants collected from WT and AdipoGR-KO mice either treated with VEH or CORT. Glucose  
130 uptake was adapted from (24, 25). Lipogenic activity, FFA re-esterification and lipolysis were  
131 adapted from (26). Details are presented in the supplemental material section.

### 133 **Histomorphological Procedures**

134 Paraffin-embedded liver and AT were cut in 4 µm thick sections and stained with hematoxylin and  
135 eosin. Adipocyte size distribution was determined on five-to-ten fields of SCAT and GAT per  
136 section covering the entire tissue surface, at ×10 magnification (optical microscope IX83  
137 Olympus). Adipocyte quantification was performed using ImageJ software  
138 (<http://rsbweb.nih.gov/ij/>) on ~1000–5000 cells per mouse. Considering that adipocytes constituted  
139 90% of the adipose tissue volume, cell number was estimated by dividing the tissue mass by the  
140 mean volume of cells. The results are expressed as cells per gram of tissue.

### 142 **Isolation of adipose macrophages from Stromal Vascular Fraction and Flow Cytometry**

#### 143 **Analysis**

144 Macrophages were isolated from SCAT and GAT from WT and AdipoGR-KO mice treated with  
145 CORT and stained as described previously (27). Stained cells were analyzed using a Gallios flow

146 cytometer (Beckman Coulter, Inc., Villepinte, France) and data were processed using Kaluza  
147 software (Beckman Coulter).

148

149 **Statistical analysis**

150 All values are expressed as the means  $\pm$  SEM. Comparisons between animal groups were carried  
151 out using a parametric Student's *t* test or by a nonparametric Mann-Whitney-Wilcoxon's test using  
152 Prism software (Graph Pad Software, Prism 5.0, La Jolla, CA).  $\chi^2$  analysis was performed to study  
153 the statistical differences in adipocyte surface distribution. A *P* value  $< 0.05$  was considered  
154 statistically significant.

155

156

157

## 158 **Results**

159

### 160 **GR is specifically invalidated in mature adipocytes of AdipoGR-KO mice**

161 To validate our model, we measured the relative GR gene expression in subcutaneous inguinal  
162 (SCAT), gonadal (GAT), perirenal (PAT) and brown adipose tissue (BAT) of AdipoGR-KO and  
163 WT mice. We observed a partial decrease in GR transcript level (50-to-60%) restricted to all AT  
164 of AdipoGR-KO mice (**Fig S1A and S1C**). The partial reduction was due to the heterogeneity of  
165 AT, which is composed of mature adipocytes but also of a mixture of non-adipocyte cell  
166 populations (28). Analysis of the isolated adipocyte fraction from SCAT and GAT showed a nearly  
167 extinction of GR protein content in AdipoGR-KO mice compared to their littermates, confirming  
168 the GR invalidation in mature adipocytes (**Fig S1B**). As expected, gene expression of two known  
169 GR target genes (*angiotensinogen* and *11 $\beta$ -hydroxysteroid dehydrogenase type 1*, 11 $\beta$ -HSD1) was  
170 significantly decreased by 50-80 %, in accordance with GR deficiency in AT of AdipoGR-KO  
171 mice (**Fig S1D and S1A**). Finally, MR mRNA content as well as two known MR target genes  
172 (*Serum and Glucocorticoid-regulated Kinase 1*, SGK1 and *Prostaglandin D2 synthase*, PTGDS)  
173 remained unchanged (**Fig S1E and S1F**), indicating that no compensatory mechanisms through  
174 MR occurred in AT of AdipoGR-KO mice.

175

### 176 **AdipoGR-KO mice harbor increased adiposity upon corticosterone treatment**

177 AdipoGR-KO and WT mice were treated with corticosterone (CORT) or vehicle (VEH) for 4  
178 weeks. As expected, corticosterone levels measured at the light/dark transition (8 am and 8 pm)  
179 were significantly elevated in the plasma of CORT-treated mice, with a maintained daily variation  
180 but were not significantly modified between the two genotypes (**Fig S2A**). In agreement with the

181 absence of adipocyte GR and in response to CORT, we detected a strong down-regulation of GR-  
182 specific target genes (*Angiotensinogen*, *11 $\beta$ -HSD1* and *FKBP5*) in all AT of AdipoGR-KO mice  
183 (**Figure S3**). CORT treatment led to a progressive, and similar body weight gain in both genotypes  
184 throughout the 4-week exposure (**Fig 1A**). Interestingly, dual energy x-ray absorptiometry (DEXA)  
185 analysis showed a marked enhancement of fat mass correlated to a decreased lean mass in CORT-  
186 treated AdipoGR-KO mice compared to CORT-WT mice (**Fig 1B**), and confirmed by the increased  
187 SCAT, GAT and PAT mass (**Fig 1C**) and the reduced liver and skeletal muscle weight in CORT-  
188 treated AdipoGR-KO mice (**Fig 1D and 1E**). Surprisingly, despite AT expansion, leptin plasma  
189 displayed a 2-fold decrease in CORT-treated AdipoGR-KO *versus* WT mice (**Fig S2B**). Analysis  
190 of food intake, locomotor activity and energy expenditure did not show any differences between  
191 both CORT-treated genotypes (**Fig S2C, S2D and S2E**). Although the respiratory exchange ratio  
192 (RER) was not modified over 24 hours, CORT-treated AdipoGR-KO mice preferentially used  
193 glucose as substrate during the dark period and switched towards fatty acid (FA) utilization during  
194 the light period (**Fig 1F right panel**), which indicated a lower FA oxidation during the night period  
195 and a higher FA utilization in the daylight period (**Fig S2F**).

196

### 197 **AdipoGR-KO mice are protected from CORT-induced glucose intolerance and insulin** 198 **resistance**

199 We next evaluated the impact of adipocyte GR invalidation on glucose and insulin tolerance in  
200 CORT- and VEH-treated mice (**Fig 2A**). As expected in WT mice, CORT treatment led to glucose  
201 intolerance and insulin resistance compared to VEH-treated mice (**Fig 2A and 2B right panel**).  
202 Interestingly, AdipoGR-KO mice showed a trend towards improved glucose tolerance and a  
203 significant increase in insulin sensitivity upon CORT treatment (**Fig 2A and 2B**). In agreement

204 with these results, CORT dramatically increased plasma insulin concentration in WT mice, but at  
205 a much lower level in AdipoGR-KO mice at 0 and 15 minutes after glucose gavage (**Fig 2C**).  
206 HOMA-IR index was significantly decreased in both CORT- and VEH-treated AdipoGR-KO mice  
207 (**Fig 2D**). Insulin signaling was also assessed upon insulin pulse experiments in tissues from both  
208 genotypes (**Fig 2E and 2F**). Interestingly, in CORT-treated AdipoGR-KO mice, Akt  
209 phosphorylation was significantly increased in the GAT and to a lesser extent in the SCAT  
210 compared to CORT-treated WT. While Akt phosphorylation was only modestly affected in AT and  
211 muscle from CORT-treated WT mice, it was markedly decreased in liver. This impaired Akt  
212 phosphorylation was not rescued in AdipoGR-KO mice suggesting that adipocyte GR invalidation  
213 specifically improves insulin signaling activation in SCAT and GAT (**Fig 2E and 2F**).

214

#### 215 **Metabolic improvement in AdipoGR-KO mice is associated with M2-like macrophage** 216 **polarization in AT**

217 In the context of obesity, insulin resistance is associated with a low-grade tissue-specific  
218 inflammation state (29, 30). GC treatment during high-fat diet induces adipose mass expansion and  
219 insulin resistance without increasing inflammation and macrophage recruitment (31). We analyzed  
220 mRNA content of key cytokines in isolated adipocyte fractions from SCAT and GAT of CORT-  
221 treated mice (**Fig S4**) and did not observe any significant changes in gene expression of anti-  
222 inflammatory cytokines (IL-10 and IL-1Ra, known to antagonize IL-1 action) (**Fig S4A**) and of  
223 pro-inflammatory IL-6, IL-1 $\beta$  in AT of both genotypes (**Fig S4B**) except for TNF $\alpha$ , which showed  
224 a trend towards a decreased expression in GAT of AdipoGR-KO mice (**Fig S4B**). Interestingly, the  
225 MCP-1 chemokine (also known as CCL2) expression was highly increased in adipocyte fractions  
226 of SCAT and GAT in AdipoGR-KO mice (**Fig S4C**), suggesting an enhanced

227 monocyte/macrophage migration and infiltration into AT. This result prompted us to measure by  
228 flow cytometry the percentage of total macrophage population in SCAT and GAT of CORT-treated  
229 AdipoGR-KO and control mice. As observed in **Figure 3A**, the percentage of F4/80+/CD11b+  
230 macrophages was not significantly altered in AdipoGR-KO compared to WT mice. We next  
231 determined M1-like macrophage population using CD11c and NOS2 markers and M2-like  
232 macrophages with the CD206 marker. Interestingly, deletion of GR in AT was associated with a  
233 significant reduction in M1-like markers and an increase in M2-like marker in SCAT of AdipoGR-  
234 KO (**Fig 3B and 3C, left panels**). In GAT of AdipoGR-KO mice, only an induction of M2-like  
235 macrophages was observed (**Fig 3B and 3C, right panels**). Interestingly, this macrophage  
236 polarization pattern was associated with a significant increase in the mRNA and protein content of  
237 adiponectin, which could exert anti-inflammatory and insulin-sensitizing properties in AT of  
238 AdipoGR-KO mice (**Fig S5**). Altogether, these results suggest that adipocyte GR invalidation may  
239 favor a M2-like macrophage phenotype in the expanded AT.

#### 240

#### 241 **Adipose GR deficiency is associated with increased lipid storage and decreased lipid**

#### 242 **mobilization**

243 Increased adiposity and metabolic changes were mostly observed in mice under CORT exposure.  
244 We thus examined the regulation of key enzymes and transcription factors involved in lipid  
245 metabolism under nutritional manipulations. Upon refeeding, two main transcription factors  
246 SREBP1c and ChREBP mediate the insulin and glucose action on enzymes of the lipogenic  
247 pathway (32-34). *SREBP1c* gene expression was significantly increased in SCAT and GAT of  
248 AdipoGR-KO mice, whereas *ChREBP* expression decreased but not significantly (**Fig 4A and 4B**).  
249 Interestingly, the expression of their target genes involved in esterification and triglycerides (TG)  
250 synthesis (*mGPAT*, *AGPAT* and *DGAT*) rather than in lipogenesis were significantly enhanced in

251 both AT of AdipoGR-KO *versus* WT mice (**Fig 4A and 4B**). Under fasting conditions, we  
252 measured the expression of ATGL (adipocyte triglyceride lipase) and of HSL (hormone-sensitive  
253 lipase), the two main enzymes of the lipolytic response. HSL protein content and phosphorylation  
254 levels were not modified in AT from AdipoGR-KO compared to WT mice (**Fig 4E and 4F**). In  
255 contrast, ATGL protein content was significantly decreased in GAT of AdipoGR-KO mice (**Fig**  
256 **4E and 4F**), while gene expression remained unchanged in both AT of AdipoGR-KO mice (**Fig**  
257 **4C and 4D**). Altogether, these results suggest that these metabolic pathways could contribute to  
258 the increased adiposity of AdipoGR-KO mice.

#### 259 260 **Functional *ex vivo* characterization of GR-deficient adipose tissues reveals increased lipid** 261 **synthesis and storage under CORT treatment**

262 The phenotype of AdipoGR-KO mice prompted us to investigate the major metabolic pathways in  
263 SCAT and GAT explants. Glucose uptake and *de novo* lipogenesis were assessed in the presence  
264 or the absence of insulin (**Fig 5A-5D**). As expected, CORT inhibited insulin-stimulated glucose  
265 uptake (**Fig 5A and 5B**) and lipogenesis (**Fig 5 and 5D**) in AT of WT mice. Interestingly, a partial  
266 to complete rescue of insulin-stimulated glucose uptake and *de novo* lipogenesis was observed in  
267 AT of AdipoGR-KO mice (**Fig 5A-5D**).

268 Isoproterenol-induced acute lipolytic activity measured by glycerol release was decreased in a  
269 similar manner by CORT in WT and AdipoGR-KO mice compared to VEH-treated mice (**Fig 5E**  
270 **and 5F**). Free fatty acid (FFA) released in the media was also measured to determine the FFA re-  
271 esterified into newly synthesized triglycerides (TG) into adipocyte lipid droplets (**Fig 5G and 5H**).  
272 The FFA-to-glycerol release ratio (also called glyceroneogenic index) is an indicator of re-  
273 esterification and is equal to 3 in the absence of newly esterified TG since 3 molecules of FFA and  
274 one molecule of glycerol are released during complete TG hydrolysis (**Fig 5I and 5J**). Under

275 CORT treatment, FFA re-esterification was decreased by 40-to-60% in AT explants of WT mice  
276 compared to VEH-treated mice (**Fig 5G and 5H**) and consequently, the glyceroneogenic index was  
277 close to 3 (**Fig 5I and 5J**). In AdipoGR-KO mice AT explants, the FFA re-esterification was  
278 strongly enhanced (**Fig 5G and 5H**) and therefore, was associated to a lower glyceroneogenic  
279 index (about 2) in AT explants (**Fig 5I and 5J**).

280 To further investigate *in vivo* the role of adipocyte GR deficiency on lipid metabolism, we  
281 measured plasma levels of non-esterified fatty acids (NEFA), TG, LDL-, and HDL-cholesterol  
282 (**Table 1**). Increased TG and NEFA plasma levels by CORT treatment was significantly reduced  
283 in GR-deficient mice. Furthermore, CORT similarly enhanced LDL-cholesterol concentration in  
284 both genotypes, but only significantly increased HDL-cholesterol concentration in AdipoGR-KO  
285 mice (**Table 1**). Taken together, these results show that adipocyte GR deletion improves lipid  
286 synthesis and storage (through *de novo* FFA synthesis and re-esterification) in SCAT and GAT of  
287 AdipoGR-KO mice.

288

### 289 **Adipose GR deficiency leads to adipocyte hypertrophy specifically in gonadal adipose tissue**

290 The flexibility of AT mass is an adaptive response to overnutrition or obesigenic conditions to  
291 prevent ectopic lipid deposition and lipotoxicity in non-adipose tissues (35). We investigated the  
292 remodeling of AT by analyzing the adipose cell size distribution in SCAT and GAT of CORT-  
293 treated mice under fed and refed conditions, a condition with increased TG accumulation.

294 Despite the increased fat mass in AdipoGR-KO mice (**Fig 1C**), the adipose cell size distribution  
295 was similar in the SCAT of AdipoGR-KO and control mice (**Fig 6A and 6C**). A similar mean  
296 adipocyte surface area and number of cells per gram of SCAT was determined on fed or refed  
297 conditions (**Fig S6A and S6B**). Analysis of GAT cell size frequency revealed clear changes  
298 depending on nutritional status in AdipoGR-KO mice (**Fig 6B and 6D**). While a similar cell size

299 distribution was observed between both genotypes under fed condition, AdipoGR-KO mice  
300 displayed a higher frequency of large adipocytes in the refed condition (**Fig 6B**), which was  
301 correlated with an increase in the mean adipocyte area and consequently a lower number of  
302 adipocyte cells per gram of GAT compared to refed-WT mice (**Fig S6A and S6B**). Finally, we did  
303 not observe any significant change in gene expression of key adipogenic transcription factors  
304 (*C/EBP $\beta$* , *C/EBP $\delta$* , *C/EBP $\alpha$*  and *PPAR $\gamma$* ) neither in SCAT nor GAT of both genotypes (**Fig S7**)  
305 indirectly suggesting that the differentiation process could be attenuated, allowing a massive  
306 enlargement of the adipocytes present in the GAT of the AdipoGR-KO refed mice.

307

### 308 **AdipoGR-KO mice are protected from CORT-induced fatty liver**

309 Chronic exposure to GCs is strongly associated with fatty liver development (36). Accordingly,  
310 numerous and large lipid droplets were revealed in liver sections of CORT-treated WT mice and  
311 correlated with a strong TG content compared to VEH-treated mice (**Fig 7A and 7B**). Interestingly,  
312 CORT-treated AdipoGR-KO mice displayed a sharp decrease in hepatic TG concentrations, similar  
313 to VEH-treated mice and was in agreement with the reduced liver weight (**Fig 7A-7B and Fig 1D**).  
314 Furthermore, no remarkable difference in the expression of key enzymes involved in lipid and  
315 glucose metabolism was observed, except for *Elovl6* which was the only lipogenic gene  
316 significantly decreased in the liver of AdipoGR-KO mice (**Fig 7C**). CPT1 (*carnitine*  
317 *palmitoyltransferase 1*), an enzyme of FA oxidation, was also markedly reduced in AdipoGR-KO  
318 mice, and paralleled the decrease in plasma ketone bodies (**Fig 7D and Table 1**). Thus, these results  
319 suggest that AdipoGR-KO mice are protected from GC-induced hepatic steatosis, through a  
320 preferential storage of lipids into AT.

321

322

**323 DISCUSSION**

324 In AT, GCs are involved in pleiotropic effects, including the control of adipogenesis, lipolysis,  
325 lipogenesis, insulin sensitivity and thermogenesis (37). Endogenous or pharmacological GC excess  
326 is also associated with lipodystrophy, insulin resistance and disturbances in glucose and lipid  
327 homeostasis (8). However, despite increasing number of studies, adipocyte GR contribution to  
328 these metabolic side effects remains unclear. To uncover its role, we generated a conditional  
329 adipocyte-specific model of GR invalidation and demonstrated that adipocyte GR invalidation  
330 leads to an expansion in fat mass under corticosterone exposure associated with improved  
331 carbohydrate and lipid profiles. Moreover, AdipoGR-KO mice exhibited enhanced insulin  
332 sensitivity, selectively restricted to AT. The main finding of our study is that adipocyte GR is a  
333 major determinant of AT expansion and is a key mediator of GC-induced metabolic dysregulations.

334 To our knowledge, only two studies have investigated the effects of GC administration on the  
335 metabolic phenotype of mice with a constitutive adipocyte GR invalidation model using either  
336 corticosterone (18) or dexamethasone (18, 20). Although very similar animal models were used,  
337 the metabolic phenotype diverged between both studies. A corticosterone treatment (10 mg/ kg of  
338 body weight in tap water) was used by Bose *et al* (18) to mimic hypercorticism conditions.  
339 Metabolic phenotyping of AdipoGR-KO mice showed no difference in weight gain, fat pad weight,  
340 hepatic TG content and glucose tolerance as well as insulin resistance compared to WT mice. These  
341 mice were treated with three times less CORT dose than our mice (30 mg/ kg of body weight in  
342 tap water), and treatment started at the age of 6 months against 3.5 months in our study. Thus low-  
343 dose of CORT on older animals may account for the lack of marked metabolic effects. Bose *et al*  
344 (18) and Shen *et al* (20) also treated their mice with dexamethasone, a specific synthetic GR agonist,  
345 but leading to conflicting results. While Bose *et al* (18) showed no major impact of dexamethasone

346 treatment (10 mg/kg per day for 2 weeks on 6-month-old mice) on adiposity and metabolic profile  
347 on adipocyte GR-deleted mice (18), Shen *et al* reported a trend towards increased adiposity with  
348 an improved glucose tolerance and insulin sensitivity in their GR-KO mice compared to WT mice  
349 following GC exposure. Akt phosphorylation was specifically enhanced in skeletal muscle of  
350 AdipoGR-KO mice. These mice were treated with lower doses of dexamethasone (3 mg/kg body  
351 weight for 2 months on 4-month-old mice) (20). The explanations for these discrepancies may rely  
352 on the treatment modalities (dose of dexamethasone, treatment duration, age of animals), which  
353 differ between the two studies. In the present study, AdipoGR-KO mice exhibited obvious  
354 increased adiposity of all fat depots associated with improved insulin sensitivity. In contrast to the  
355 study of Shen *et al.* (20) which reported an increased insulin sensitivity restricted to skeletal muscle,  
356 we clearly demonstrated that GR deletion in adipocytes improved this signalling pathway  
357 selectively in AT. This suggests that adipocyte GR could represent an important determinant of  
358 whole body insulin sensitivity in AdipoGR-KO mice. A key explanation for these tissue-specific  
359 modulations in insulin sensitivity could be related to our choice of a conditional model of GR-  
360 invalidation, which allowed us to circumvent the phenotypic impact of GR ablation during AT  
361 growth and development. Since several studies have documented that GCs and the GR are key  
362 players of adipose physiology (8), constitutive GR invalidation models used in the previously  
363 published works (16-20) could combine GR pleiotropic effects on both developmental and  
364 metabolic functions of adipocytes.

365 It is well established that GCs actions are mediated through GR and MR in AT of rodents. GCs  
366 affinity for the MR is ten-fold higher than for GR (38), and MR gene expression is known to be  
367 elevated in AT of obese rodents (38, 39). In agreement with Shen *et al.* (20), we did not find any  
368 upregulation of MR mRNA levels nor any of its target genes (SGK1 and PTGDS) in AT of our

369 mice suggesting that no adaptive mechanism through the MR pathway was observed in our GR  
370 deficient mice.

371 Rodent and human obesity are associated with a sub-inflammatory state of AT, with pro-  
372 inflammatory M1 macrophage infiltration (40, 41). In this context, the effects of GCs seem  
373 paradoxical since they induce an AT expansion and disorders in glucose and lipid metabolism, but  
374 also exert potent anti-inflammatory properties (31). In our study, adipocyte GR deletion did not  
375 influence the total number of macrophages, but modulated macrophage polarization in a depot-  
376 dependent manner. The global shift from M1 to M2 macrophage polarization observed in SCAT  
377 and in a less pronounced manner in GAT, fits with the improved metabolic profile of AdipoGR-  
378 KO mice, and suggests that the absence of adipocyte GR protects from an inflammatory phenotype  
379 and the GC-induced related metabolic complications. What could be the mechanisms underlying  
380 these changes in macrophage polarization in GC-treated AdipoGR-KO mice? Several arguments  
381 are in favour of a M2-like shift of macrophage polarization in the AT of AdipoGR-KO mice  
382 following CORT exposure. First, the enhanced local adiponectin mRNA and protein content in  
383 SCAT and GAT of AdipoGR-KO mice may participate to the anti-inflammatory profile in AT and  
384 to the specific improvement in AT insulin sensitivity (42). Second, despite the expansion of AT,  
385 AdipoGR-KO mice exhibited a 2-fold decrease in leptin plasma levels. This is in agreement with  
386 the known direct effect of GCs to increase leptin synthesis and secretion in adipocytes (43). Leptin  
387 modulates a wide range of immune and inflammatory processes, activating monocyte proliferation  
388 and cytokine/chemokine expression (44, 45), macrophage phagocytosis and chemotaxis (46). Thus,  
389 under GC exposure, the lower leptin levels in AdipoGR-KO mice could mitigate macrophage  
390 classical activation and promote a M2 alternative phenotype. Alternatively, due to the increased  
391 lipid esterification and synthesis, AdipoGR-KO mice exhibited lower NEFA plasma levels, which

392 are also known to promote M1 polarization (47). Consequently, decreased NEFA and leptin levels  
393 could act in synergy to favour M2 polarization. This illustrates the possibility that expansion of AT  
394 could be associated with a prominent M2-like macrophage phenotype, together with a healthier  
395 metabolic profile.

396 In our work, several results converge to demonstrate that the adipocyte GR is a major determinant  
397 of AT expandability. First, at a morphological level, the adipocyte GR deletion was associated with  
398 an increased fat deposition. Interestingly, a higher proportion of large adipocytes in AdipoGR-KO  
399 fat mass was only detectable upon refeeding nutritional manipulation, and in a depot-specific  
400 manner since GAT seemed more prone to these genotype-associated cell size variations. Second,  
401 these morphological changes were paralleled by biochemical changes that fit with the increased  
402 insulin sensitivity in AdipoGR-KO mice despite CORT exposure. Experiments performed on  
403 SCAT or GAT explants showed a total or partial rescue of glucose uptake and *de novo* lipogenesis  
404 in CORT-treated AdipoGR-KO animals, which was in agreement with the increased expression of  
405 genes targeted by the key lipogenic transcription factor SREBP1c. Surprisingly, despite  
406 unmodified isoproterenol-stimulated lipolysis in adipose explants from CORT-treated AdipoGR-  
407 KO mice, FFA re-esterification was clearly induced, participating to lipid storage into adipocytes  
408 and improved plasma lipid profile. All these biochemical events could reflect the combined effect  
409 of the increased insulin sensitivity in AT but also of the absence of GR-mediated actions on its  
410 target genes (48). Finally, at a systemic level, adipocyte GR deletion is also characterized by  
411 changes in fuel utilization, as assessed by circadian variations in respiratory exchange ratio (RER).  
412 The increased preferential carbohydrate oxidation observed in AdipoGR-KO mice mainly occurred  
413 during the dark period. Consequently, this carbohydrate utilization improves glucose homeostasis.  
414 The reorientation of glucose utilization towards AT in AdipoGR-KO mice is sufficient to totally

415 prevent liver steatosis induced by CORT and may protect other non-adipose tissues from lipid spill  
416 over. Thus, adipocyte GR could play a key role in the onset and progression of GC-induced liver  
417 steatosis.

418 In conclusion, our results demonstrate that a conditional adipose-specific GR invalidation protects  
419 from insulin resistance induced by GCs. This is in close relationship with a specific improvement  
420 in AT insulin sensitivity, that favours an expansion of fat depots. The AdipoGR-KO mouse thus  
421 represents a model of AT overexpansion associated with a healthier metabolic phenotype.  
422 Furthermore, this strongly suggests that adipocyte GR is a limiting factor for AT expansion,  
423 contributing to metabolic disorders under GC exposure. A selective modulation of adipocyte GR  
424 expression and/or function is thus a relevant target to counteract the metabolic side effects of GCs.

425

426

427 **ACKNOWLEDGEMENTS**

428 We thank Dr Offermanns (Bad Nauheim, Germany) and Dr Tronche (Paris, France) for their kind  
429 gift of AdipoqCRE-ERT2 and GRlox/lox mice, respectively. The authors are grateful to Dr F.  
430 Benhamed (INSERM 1016, UMR8104, Paris), M. Auclair, C. Kazazian, R. Tchuinkam and G.  
431 Vacher for their technical assistance. We thank L. Dinard, A. Guyomard, T. Coulais, Q. Pointout  
432 (animal housing facility), S. Dumont, B. Solhonne and F. Merabtene (Histomorphology platform,  
433 Sorbonne University-INSERM, UMS 30, Paris), R. Morrichon (Cell imaging and confocal  
434 microscopy platform, Sorbonne University-INSERM, UMS 30, Paris) and A. Munier (Cytometry  
435 platform, Sorbonne University-INSERM, UMS30, Paris) for their excellent work. C. Klein, et K.  
436 Garbin for technical and imaging support (CHIC platform, Centre de Recherche des Cordeliers,  
437 UMRS 1138). We thank Dr Alexandra Grosfeld for helpful discussion.

438 **Funding.** This work was supported by grants from INSERM, Sorbonne University, French Society  
439 of Diabetes (Johnson & Johnson and SFD) and the Medical Research Foundation (FRM). HD was  
440 supported by a doctoral fellowship from the Ministère de l'Enseignement Supérieur et de la  
441 Recherche and of the Medical Research Foundation (FRM). TTHD was a recipient of the French  
442 Society of Endocrinology (SFE), and the French Embassy in Vietnam. VB was a recipient of the  
443 French Society of Endocrinology (SFE).

444 **Author contributions.** MM, BF designed the research; HD, MG, BA, VB, TTHD, MB, AL, CM,  
445 CP, MM performed the research; TL contributed to generate the AdipoGR-KO mouse model and  
446 animal experiments; RGD and SL performed indirect calorimetry measurements and analyzed data;  
447 HD, MG, BA, BF, MM analyzed data; HD, BF, MM wrote the paper. MM and BF are the  
448 guarantors of this work and, as such, have full access to all the data in the study and take  
449 responsibility for the integrity of the data and the accuracy of the data analysis.

450 **Duality of Interest.** The authors declare no conflict of interest.

451

452 **REFERENCES**

- 453 1. Quax RA, Manenschijn L, Koper JW, Hazes JM, Lamberts SW, Van Rossum EF, Feelders  
454 RA. Glucocorticoid sensitivity in health and disease. *Nat Rev Endocrinol* 2013;9: 670-686
- 455 2. Fox CS, Massaro JM, Hoffmann U, Pou KM, Maurovich-Horvat P, Liu CY, Vasan RS,  
456 Murabito JM, Meigs JB, Cupples LA, D'agostino RBS, O'donnell CJ. Abdominal visceral and  
457 subcutaneous adipose tissue compartments: association with metabolic risk factors in the  
458 Framingham Heart Study. *Circulation* 2007;116: 39-48
- 459 3. Tran TT, Yamamoto Y, Gesta S, Kahn CR. Beneficial effects of subcutaneous fat  
460 transplantation on metabolism. *Cell Metab* 2008;7: 410-420
- 461 4. Friedman TC, Mastorakos G, Newman TD, Mullen NM, Horton EG, Costello R,  
462 Papadopoulos NM, Chrousos GP. Carbohydrate and lipid metabolism in endogenous  
463 hypercortisolism: shared features with metabolic syndrome X and NIDDM. *Endocr J* 1996;43: 645-  
464 655
- 465 5. Campbell JE, Peckett AJ, D'souza AM, Hawke TJ, Riddell MC. Adipogenic and lipolytic  
466 effects of chronic glucocorticoid exposure. *Am J Physiol Cell Physiol* 2011;300: 198-209
- 467 6. Ayala-Sumano JT, Velez-Delvalle C, Beltrán-Langarica A, Marsch-Moreno M,  
468 Hernandez-Mosqueira C, Kuri-Harcuch W. Glucocorticoid paradoxically recruits adipose  
469 progenitors and impairs lipid homeostasis and glucose transport in mature adipocytes. *Sci Rep*  
470 2013;3: 2573
- 471 7. Zennaro MC, Caprio M, Fève B. Mineralocorticoid receptors in the metabolic syndrome.  
472 *Trends Endocrinol Metab* 2009;20: 444-451
- 473 8. Lee MJ, Pramyothin P, Karastergiou K, Fried SK. Deconstructing the roles of  
474 glucocorticoids in adipose tissue biology and the development of central obesity. *Biochim Biophys*  
475 *Acta* 2014;1842: 473-481
- 476 9. Ottosson M, Vikman-Adolfsson K, Enerbäck S, Olivecrona G, Björntorp P. The effects of  
477 cortisol on the regulation of lipoprotein lipase activity in human adipose tissue. *J Clin Endocrinol*  
478 *Metab* 1994;79: 820-825
- 479 10. Sul HS, Latasa MJ, Moon Y, Kim K-Y. Regulation of the Fatty Acid Synthase Promoter  
480 by Insulin. *J Nutr* 2000;130: 3155-3205
- 481 11. Peckett AJ, Wright DC, Riddell MC. The effects of glucocorticoids on adipose tissue lipid  
482 metabolism. *Metabolism* 2011;60: 1500-1510
- 483 12. Kuhn E, Bourgeois C, Keo V, Viengchareun S, Muscat A, Meduri G, Le Menuet D, Fève  
484 B, Lombès M. Paradoxical resistance to high-fat diet-induced obesity and altered macrophage  
485 polarization in mineralocorticoid receptor-overexpressing mice. *Am J Physiol Endocrinol Metab*  
486 2014;306: E75-90
- 487 13. Urbanet R, Nguyen Dinh Cat A, Feraco A, Venteclef N, El Mogrhabi S, Sierra-Ramos C,  
488 Alvarez De La Rosa D, Adler GK, Quilliot D, Rossignol P, Fallo F, Touyz RM, Jaisser F.  
489 Adipocyte Mineralocorticoid Receptor Activation Leads to Metabolic Syndrome and Induction of  
490 Prostaglandin D2 Synthase. *Hypertension* 2015;66: 149-157
- 491 14. Guo C, Ricchiuti V, Lian BQ, Yao TM, Coutinho P, Romero JR, Li J, Williams GH, Adler  
492 GK. Mineralocorticoid receptor blockade reverses obesity-related changes in expression of  
493 adiponectin, peroxisome proliferator-activated receptor-gamma, and proinflammatory adipokines.  
494 *Circulation* 2008;117: 2253-2261
- 495 15. Takeshita Y, Watanabe S, Hattori T, Nagasawa K, Matsuura N, Takahashi K, Murohara T,  
496 Nagata K. Blockade of glucocorticoid receptors with RU486 attenuates cardiac damage and  
497 adipose tissue inflammation in a rat model of metabolic syndrome. *Hypertens Res* 2015;38: 741-  
498 750

- 499 16. De Kloet AD, Krause EG, Solomon MB, Flak JN, Scott KA, Kim DH, Myers B, Ulrich-  
500 Lai YM, Woods SC, Seeley RJ, Herman JP. Adipocyte glucocorticoid receptors mediate fat-to-  
501 brain signaling. *Psychoneuroendocrinology* 2015;56: 110-119
- 502 17. Desarzens S, Faresse N. Adipocyte glucocorticoid receptor has a minor contribution in  
503 adipose tissue growth. *J Endocrinol* 2016;230: 1-11
- 504 18. Bose SK, Hutson I, Harris CA. Hepatic Glucocorticoid Receptor Plays a Greater Role Than  
505 Adipose GR in Metabolic Syndrome Despite Renal Compensation. *Endocrinology* 2016;157:  
506 4943-4960
- 507 19. Mueller KM, Hartmann K, Kaltenecker D, Vettorazzi S, Bauer M, Mauser L, Amann S, Jall  
508 S, Fischer K, Esterbauer H, Müller TD, Tschöp MH, Magnes C, Haybaeck J, Scherer T, Bordag  
509 N, Tuckermann JP, Moriggl R. Adipocyte Glucocorticoid Receptor Deficiency Attenuates Aging-  
510 and HFD-Induced Obesity and Impairs the Feeding-Fasting Transition. *Diabetes* 2017;66: 272-286
- 511 20. Shen Y, Roh HC, Kumari M, Rosen ED. Adipocyte glucocorticoid receptor is important in  
512 lipolysis and insulin resistance due to exogenous steroids, but not insulin resistance caused by high  
513 fat feeding. *Mol Metab.* 2017;6: 1150-1160
- 514 21. Tronche F, Kellendonk C, Kretz O, Gass P, Anlag K, Orban PC, Bock R, Klein R, Schütz  
515 G. Disruption of the glucocorticoid receptor gene in the nervous system results in reduced anxiety.  
516 *Nat Genet* 1999;23: 99-103
- 517 22. Sassmann A, Offermanns S, Wettschureck N. Tamoxifen-inducible Cre-mediated  
518 recombination in adipocytes. *Genesis* 2010;48: 618-625
- 519 23. Karatsoreos IN, Bhagat SM, Bowles. N.P., Weil ZM, Pfaff DW, Mcewen BS. Endocrine  
520 and physiological changes in response to chronic corticosterone: a potential model of the metabolic  
521 syndrome in mouse. *Endocrinology* 2010;151: 2117-2127
- 522 24. Rogers PM, Mashtalir N, Rathod MA, Dubuisson O, Wang Z, Dasuri K, Babin S, Gupta A,  
523 Markward N, Cefalu WT, Dhurandhar NV. Metabolically favorable remodeling of human adipose  
524 tissue by human adenovirus type 36. *Diabetes* 2008;57: 2321-2331
- 525 25. Attané C, Daviaud. D., Dray C, Dusaulcy R, Masseboeuf M, Prévot D, Carpéné C, Castan-  
526 Laurell I, Valet P. Apelin stimulates glucose uptake but not lipolysis in human adipose tissue ex  
527 vivo. *J Mol Endocrinol* 2011;46: 21-28
- 528 26. Tordjman J, Chauvet G, Quette J, Beale EG, Forest C, Antoine B. Thiazolidinediones block  
529 fatty acid release by inducing glyceroneogenesis in fat cells.  
530 Tordjman J1, Chauvet G, Quette J, Beale EG, Forest C, Antoine B. *J Biol Chem* 2003;278: 18785-  
531 18790
- 532 27. Martinerie C, Garcia M, Do TT, Antoine B, Moldes M, Dorothee G, Kazazian C, Auclair  
533 M, Buyse M, Ledent T, Marchal PO, Fesatidou M, Beisseiche A, Koseki H, Hiraoka S,  
534 Chadjichristos CE, Blondeau B, Denis RG, Luquet S, Fève B. NOV/CCN3: A New Adipocytokine  
535 Involved in Obesity-Associated Insulin Resistance. *Diabetes* 2016;65: 2502-2515
- 536 28. Lee MJ, Wu Y, Fried SK. Adipose Tissue Heterogeneity: Implication of depot differences  
537 in adipose tissue for Obesity Complications. *Mol Aspects Med* 2013;34: 1-11
- 538 29. Chen L, Chen R, Wang H, Liang F. Mechanisms Linking Inflammation to Insulin  
539 Resistance. *Int J Endocrinol* 2015;2015: 1-9
- 540 30. Rehman K, Akash MS. Mechanisms of inflammatory responses and development of insulin  
541 resistance: how are they interlinked? *J Biomed Sci* 2016;23: 87
- 542 31. Patsouris D, Neels JG, Fan W, Li P-P, Nguyen NTA, Olefsky JM. Glucocorticoids and  
543 Thiazolidinediones Interfere with Adipocyte-mediated Macrophage Chemotaxis and Recruitment.  
544 *J Biol Chem* 2009;284: 31223-31235

- 545 32. Eberlé D, Hegarty B, Bossard P, Ferré P, Foufelle F. SREBP transcription factors: master  
546 regulators of lipid homeostasis. *Biochimie* 2004;86: 839-848
- 547 33. Herman MA, Peroni OD, Villoria J, Schön MR, Abumrad NA, Blüher M, Klein S, Kahn  
548 BB. A novel ChREBP isoform in adipose tissue regulates systemic glucose metabolism. *Nature*  
549 2012;484: 333-338
- 550 34. Abdul-Wahed A, Guilmeau S, Postic C. Sweet Sixteenth for ChREBP: Established Roles  
551 and Future Goals. *Cell Metab* 2017;26: 324-341
- 552 35. Rutkowski JM, Stern JH, Scherer PE. The cell biology of fat expansion. *J Cell Biol*  
553 2015;208: 501-512
- 554 36. Andrews RC, Walker BR. Glucocorticoids and insulin resistance: old hormones, new  
555 targets. *Clin Sci (Lond)* 1999;96: 513-523
- 556 37. Ferràu F, Korbonits M. Metabolic comorbidities in Cushing's syndrome. *Eur J Endocrinol*  
557 2015;173: M133-157
- 558 38. Arriza JL, Weinberger C, Cerelli G, Glaser TM, Handelin BL, Housman DE, Evans RM.  
559 Cloning of human mineralocorticoid receptor complementary DNA: structural and functional  
560 kinship with the glucocorticoid receptor. *Science* 1987;237: 268-275
- 561 39. Hirata A, Maeda N, Hiuge A, Hibuse T, Fujita K, Okada T, Kihara S, Funahashi T,  
562 Shimomura I. Blockade of mineralocorticoid receptor reverses adipocyte dysfunction and insulin  
563 resistance in obese mice. *Cardiovasc Res* 2009;84: 164-172
- 564 40. Lumeng CN, Bodzin JL, Saltiel AR. Obesity induces a phenotypic switch in adipose tissue  
565 macrophage polarization. *J Clin Invest* 2007;117: 175-184
- 566 41. Herrero L, Shapiro H, Nayer A, Lee J, Shoelson SE. Inflammation and adipose tissue  
567 macrophages in lipodystrophic mice. *Proc Natl Acad Sci U S A* 2010;107: 240-245
- 568 42. Mandal P, Pratt BT, Barnes M, McMullen MR, Nagy LE, Molecular mechanism for  
569 adiponectin-dependent M2 macrophage polarization link between the metabolic and innate  
570 immune activity of full-length adiponectin. *J Biol Chem* 2011;286:13460-13469
- 571 43. Sliker LJ, Sloop KW, Surface PL, Kriauciunas A, Laquier F, Manetta J, Bue-Valleskey J,  
572 Stephens TW. Regulation of expression of ob mRNA and protein by glucocorticoids and cAMP. *J*  
573 *Biol Chem* 1996;271: 5301-5304
- 574 44. Santos-Alvarez J, Goberna R, Sánchez-Margalet V. Human leptin stimulates proliferation  
575 and activation of human circulating monocytes. *Cell Immunol* 1999;194: 6-11
- 576 45. Tsiotra PC, Boutati E, Dimitriadis G, Raptis SA. High insulin and leptin increase resistin  
577 and inflammatory cytokine production from human mononuclear cells. *Biomed Res Int* 2013;2013:  
578 487081
- 579 46. Gruen ML, Hao M, Piston DW, Hasty AH. Leptin requires canonical migratory signaling  
580 pathways for induction of monocyte and macrophage chemotaxis. *Am J Physiol Cell Physiol*  
581 2007;293: C1481-1488
- 582 47. Shi H, Kokoeva MV, Inouye K, Tzameli I, Yin H, Flier JS. TLR4 links innate immunity  
583 and fatty acid-induced insulin resistance. *J Clin Invest* 2006;116: 3015-3025
- 584 48. Wang JC, Gray NE, Kuo T, Harris CA. Regulation of triglyceride metabolism by  
585 glucocorticoid receptor. *Cell Biosci* 2012;2: 19
- 586

587

588

589

590

591

592 **Table 1: Metabolic parameters of control and CORT-treated mice**

Plasma metabolic parameters	VEH		CORT	
	<i>WT</i>	<i>AdipoGR-KO</i>	<i>WT</i>	<i>AdipoGR-KO</i>
HDL-Chol (mg/dL)	48.9 ± 11.3	44.1 ± 9.3	46.3 ± 10.3	58.9 ± 12.9 *
LDL-Chol (mg/dL)	48.6 ± 12.9	16.1 ± 4.1 **	85.5 ± 26.0 #	108.4 ± 25.4 ##
TG (μM)	348.9 ± 18.5	320.4 ± 27.6	477.2 ± 26.9 ##	400.5 ± 18.1 *#
NEFA (μM)	479.6 ± 45.4	432.2 ± 42.9	653.7 ± 39.2 #	437.0 ± 52.8 *
Ketone bodies (mmol/mL)	-	-	0.93 ± 0.12	0.48 ± 0.07 *

593

594

595 Following a 4-week exposure to VEH or CORT, mice were sacrificed. Plasma samples were  
 596 collected from overnight fasted mice and then examined for the indicated metabolic parameters.

597 Results represent means ± SEM (n=4-9). \*  $P < 0.05$ ; \*\*  $P < 0.01$ , *AdipoGR-KO versus WT* mice;

598 #  $P < 0.05$ ; ##  $P < 0.01$ , *CORT versus control (VEH)* mice.

599

600

601

602

603 **Legends**

604

605 **Figure 1: Adipocyte GR deficiency leads to an increased adiposity under corticosterone**  
606 **treatment**

607 Eighteen-week-old mice were analyzed after a 4-week exposure to vehicle (VEH) or  
608 corticosterone (CORT). **(A)** Mice body weight gain during the 4-week-treatment (n=12/group). **(B)**  
609 Fat and lean body mice composition as determined by DEXA analyzer of WT and AdipoGR-KO  
610 mice (n=6/group). **(C-E)** Mice tissues were dissected and weighted. Subcutaneous (SCAT),  
611 gonadal (GAT) and perirenal (PAT) adipose tissues **(C)**, liver **(D)** and posterior leg skeletal muscles  
612 **(E)** weight are presented as percentage of total body weight of AdipoGR-KO and WT mice (n=6-  
613 12/group). **(F, left panel)** Respiratory exchange ratio (RER) measured by calculating oxygen  
614 consumption and carbon dioxide production over a 24-hour period in CORT-treated WT and  
615 AdipoGR-KO mice through an indirect calorimetry apparatus. **(F, right panel)** Mean of RER  
616 presented 24-h period or per 12-h period of daylight or night (n=6/group). Data are presented as  
617 the mean +/- SEM; \*  $P < 0.05$ ; \*\*  $P < 0.01$ ; \*\*\*  $P < 0.001$ , for AdipoGR-KO *versus* WT mice. #  $P$   
618  $< 0.05$ ; ##  $P < 0.01$ , for CORT *versus* VEH-treatment.

619

620

621 **Figure 2: Adipocyte GR deficiency improves insulin sensitivity specifically in adipose tissues**  
622 **of CORT-treated mice**

623 Dynamic tests were performed on 18-week-old mice treated either with VEH or CORT for 4-weeks  
624 (n=12/group). **(A)** For OGTT, glucose was administrated by oral gavage (1 g/kg body weight) in 5  
625 h-fasted mice. Glycemia was determined at indicated times (left panel). Area under the curve  
626 (AUC) of the OGTT is presented on the right panel. **(B)** For ITT, insulin was administrated by I.P.

627 injection (1 UI/kg body weight) in 5 h-fasted mice. Glucose levels were determined at indicated  
628 times (left panel) and AUC presented on the right panel. (C) Plasma insulin levels were obtained  
629 from whole-tail vein blood sampled at baseline and 15 min after glucose administration. (D)  
630 HOMA-IR index was calculated from fasting insulin and fasting glucose levels. (E-F) Insulin pulse  
631 was performed on mice after VEH or CORT exposure. Mice were I.P. injected by 1.5 UI/kg of  
632 insulin and sacrificed 10 minutes later. Representative Western Blots (E) and quantifications (F)  
633 of insulin-stimulated phosphorylation of Akt/total Akt in SCAT and GAT adipose tissues, liver and  
634 skeletal muscle of AdipoGR-KO and WT mice (n=6/group). Data represent the mean +/- SEM; \*  $P$   
635 <0.05; \*\*  $P$  <0.01, for AdipoGR-KO *versus* WT mice; #  $P$  <0.05; ##  $P$  <0.01; ###  $P$  <0.001, for  
636 CORT *versus* VEH-treatment.

637  
638 **Figure 3: Adipocyte GR deficiency favors M2-like macrophage polarization in adipose tissue**  
639 **of CORT-treated-mice**

640 (A-C) Flow cytometry analysis of macrophages isolated from SCAT and GAT of CORT-treated  
641 WT and AdipoGR-KO mice (n=6/group). (A) Percentages of F4/80+/CD11b+ macrophages in  
642 SCAT (left panel) and GAT (right panel). (B-C) Percentage of M1-like and M2-like macrophages  
643 (with CD11c/CD206 markers) (B) and of M1-like and M2-like macrophages (with NOS2/CD206  
644 markers) (C) in gated population from F4/80+/CD11b+ macrophages in SCAT (left panel) and  
645 GAT (right panel) of WT and AdipoGR-KO mice. Data represent the mean +/- SEM; \*  $P$  <0.05; \*\*  
646  $P$  <0.01, for AdipoGR-KO *versus* WT mice.

647  
648 **Figure 4: Adipocyte GR deficiency alters lipid metabolism enzymes content in adipose tissues**  
649 **of CORT-treated mice**

650 Gene expression and protein content analysis were performed on 18-week-old mice treated with  
651 CORT for 4-weeks (n=6/group). **(A-B)** Relative gene expression of key enzymes of lipogenic and  
652 esterification pathways was determined by RT-qPCR in subcutaneous (SCAT) **(A)** and gonadal  
653 (GAT) **(B)** adipose tissues of refed AdipoGR-KO and WT mice (n=6/group). **(C-D)** Relative gene  
654 expression of key enzymes of lipolysis, *ATGL* and *HSL*, determined by RT-qPCR in total SCAT  
655 and GAT of fasted AdipoGR-KO and WT mice (n=6/group). **(E-F)** A representative Western Blot  
656 (upper panel) and quantification (lower panel) of key enzymes of lipolysis: ATGL and  
657 phosphorylated HSL/total HSL ratio in SCAT **(E)** and GAT **(F)** of overnight fasted AdipoGR-KO  
658 and WT mice. The 36B4 protein was used as loading control. Data represent the mean +/- SEM; \*  
659  $P < 0.05$ ; \*\*  $P < 0.01$ , for AdipoGR-KO *versus* WT mice.

660  
661 **Figure 5: Metabolic responses of adipose tissue explants from AdipoGR-KO and WT mice**  
662 Eighteen-week-old mice were sacrificed after a 4-week exposure to VEH or CORT. Subcutaneous  
663 **(A, C, E, G, I)** and gonadal **(B, D, F, H, J)** fat pad explants were isolated and then tested for  
664 different metabolic activities as described in *Materials and Methods* (n=3-6/group). **(A-B)**  
665 Radiolabeled-2-deoxyglucose incorporation was performed in the presence or the absence of  
666 insulin (Ins, 100 nM) (n=6/group). **(C-D)** *De novo* lipogenic flux was performed in the presence or  
667 the absence of insulin (Ins, 100 nM) by using radiolabeled [<sup>14</sup>C]-glucose. Radiolabeled lipids were  
668 extracted and counted. **(E-F)** Lipolytic activity was tested in the absence or the presence of  
669 isoproterenol (IPR, 1 μM). Glycerol released into the media was measured. **(G-H)** Radiolabeled  
670 pyruvate incorporation evaluates the amount of free-fatty acids (FFA) esterified and incorporated  
671 into triglycerides (TG) during a 1-h lipolytic period. Glucose transport, lipogenesis, lipolysis and  
672 reesterification activities were expressed as nmol/mg of AT/h and then arbitrary normalized to 1

673 from VEH-treated WT mice. **(I-J)** Glyceroneogenic index measured ratio of FFA *versus* glycerol  
674 released in the culture media. FFA/glycerol values correspond to the means of the ratios determined  
675 in each animal. Data represent the mean +/- SEM; \*  $P < 0.05$ ; \*\*  $P < 0.01$ ; \*\*\*  $P < 0.001$ , for AdipoGR-  
676 KO *versus* WT mice; #  $P < 0.05$ ; ##  $P < 0.01$ ; ###  $P < 0.001$ , for CORT *versus* VEH treatment.

677  
678 **Figure 6: Adipocyte GR deficiency leads to adipocyte hypertrophy in gonadal adipose tissue**  
679 **of CORT-treated mice**

680 Eighteen-week-old mice were sacrificed after a 4-week CORT exposure under fed and refed  
681 conditions (n=3-4/group). SCAT **(A, C)** and GAT **(B, D)** fat pads from CORT-AdipoGR-KO and  
682 WT mice were isolated for histomorphological analysis as described in *Materials and Methods*.  
683 Distribution of cell surfaces was determined in AT of AdipoGR-KO and WT mice under fed **(A,**  
684 **B)** and refed **(C, D)** conditions.  $\chi^2$  analysis was carried out for statistical differences in adipocyte  
685 surface distribution between AdipoGR-KO and WT mice.

686  
687 **Figure 7: Adipose specific GR invalidation prevents CORT-induced-hepatic steatosis**

688 Eighteen-week-old mice were sacrificed after a 4-week exposure to VEH or CORT under refed  
689 and fasted conditions (n=6/group). **(A)** Hematoxylin/eosin staining of liver sections from WT and  
690 AdipoGR-KO mice and **(B)** liver TG content. **(C-D)** Relative mRNA content of key enzymes of  
691 lipid and glucose metabolism as determined by RT-qPCR in liver of refed- **(C)** and fasted- **(D)**  
692 AdipoGR-KO and WT mice. Data represent the mean +/- SEM. \*  $P < 0.05$ ; \*\*  $P < 0.01$ , for AdipoGR-  
693 KO *versus* WT mice; ##  $P < 0.01$ , for CORT *versus* VEH treatment.

694  
695

696

Figure 1

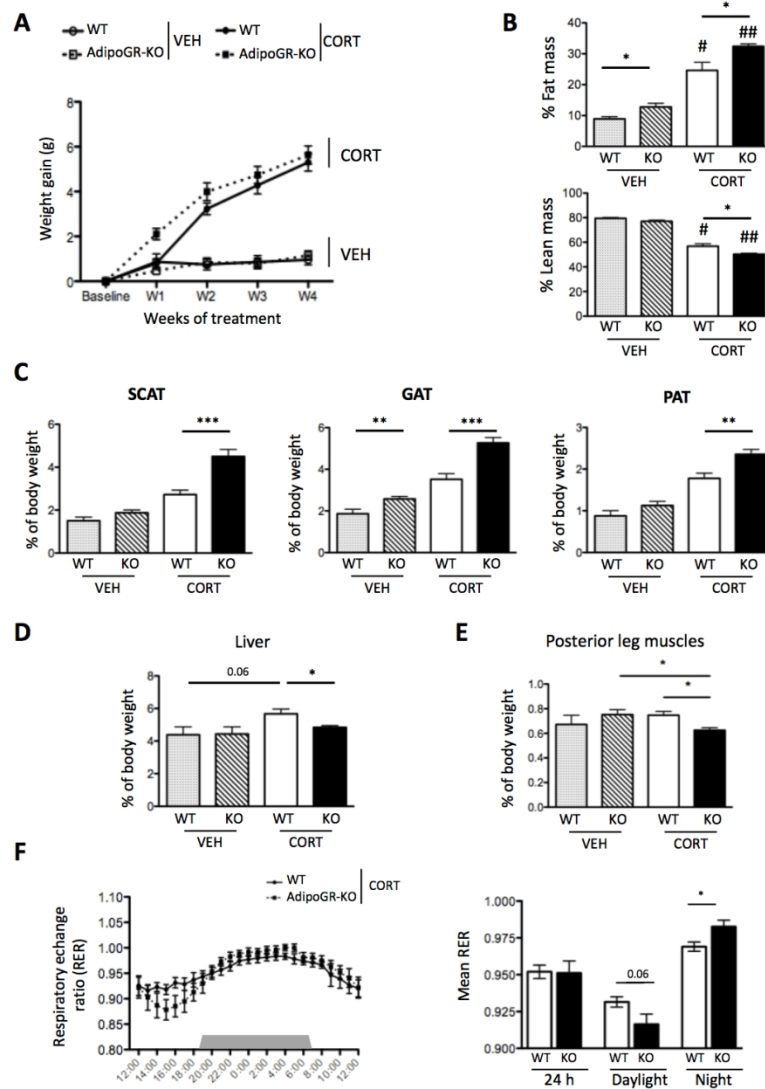


Figure 1: Adipocyte GR deficiency leads to an increased adiposity under corticosterone treatment. Eighteen-week-old mice were analyzed after a 4-week exposure to vehicle (VEH) or corticosterone (CORT). (A) Mice body weight gain during the 4-week-treatment (n=12/group). (B) Fat and lean body mice composition as determined by DEXA analyzer of WT and AdipoGR-KO mice (n=6/group). (C-E) Mice tissues were dissected and weighted. Subcutaneous (SCAT), gonadal (GAT) and perirenal (PAT) adipose tissues (C), liver (D) and posterior leg skeletal muscles (E) weight are presented as percentage of total body weight of AdipoGR-KO and WT mice (n=6-12/group). (F, left panel) Respiratory exchange ratio (RER) measured by calculating oxygen consumption and carbon dioxide production over a 24-hour period in CORT-treated WT and AdipoGR-KO mice through an indirect calorimetry apparatus. (F, right panel) Mean of RER presented 24-h period or per 12-h period of daylight or night (n=6/group). Data are presented as the mean +/- SEM; \* P < 0.05; \*\* P < 0.01; \*\*\* P < 0.001, for AdipoGR-KO versus WT mice. # P < 0.05; ## P < 0.01, for CORT versus VEH-treatment.

Figure 2

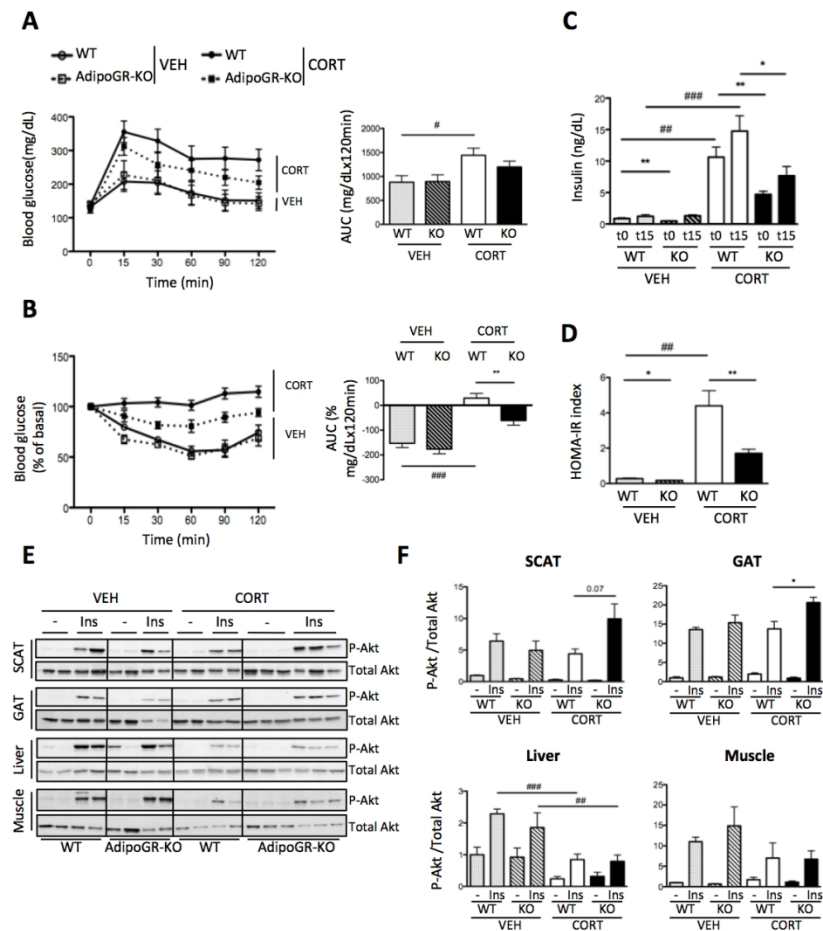


Figure 2: Adipocyte GR deficiency improves insulin sensitivity specifically in adipose tissues of CORT-treated mice. Dynamic tests were performed on 18-week-old mice treated either with VEH or CORT for 4-weeks (n=12/group). (A) For OGTT, glucose was administered by oral gavage (1 g/kg body weight) in 5 h-fasted mice. Glycemia was determined at indicated times (left panel). Area under the curve (AUC) of the OGTT is presented on the right panel. (B) For ITT, insulin was administered by I.P. injection (1 UI/kg body weight) in 5 h-fasted mice. Glucose levels were determined at indicated times (left panel) and AUC presented on the right panel. (C) Plasma insulin levels were obtained from whole-tail vein blood sampled at baseline and 15 min after glucose administration. (D) HOMA-IR index was calculated from fasting insulin and fasting glucose levels. (E-F) Insulin pulse was performed on mice after VEH or CORT exposure. Mice were I.P. injected by 1.5 UI/kg of insulin and sacrificed 10 minutes later. Representative Western Blots (E) and quantifications (F) of insulin-stimulated phosphorylation of Akt/total Akt in SCAT and GAT adipose tissues, liver and skeletal muscle of AdipoGR-KO and WT mice (n=6/group). Data represent the mean  $\pm$  SEM; \* P < 0.05; \*\* P < 0.01, for AdipoGR-KO versus WT mice; # P < 0.05; ## P < 0.01; ### P < 0.001, for CORT versus VEH-treatment.

190x275mm (150 x 150 DPI)

Figure 3

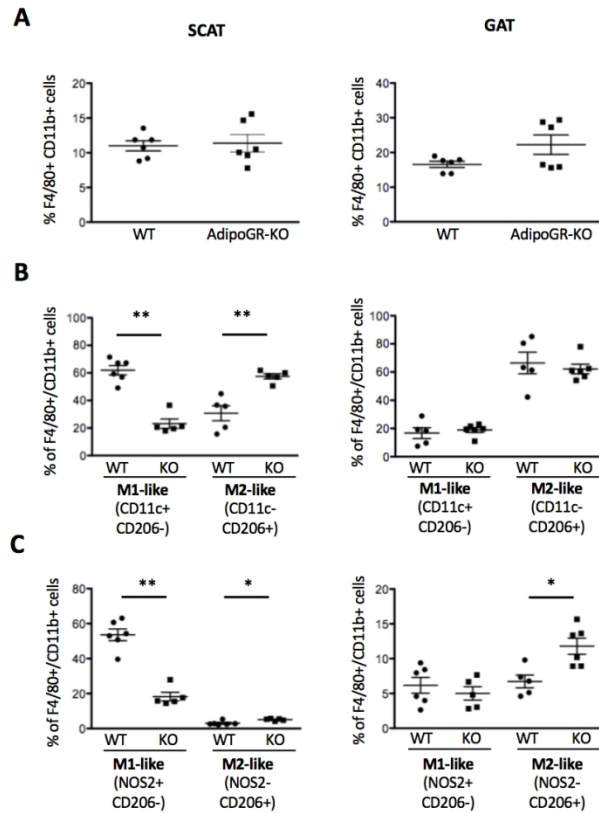


Figure 3: Adipocyte GR deficiency favors M2-like macrophage polarization in adipose tissue of CORT-treated-mice (A-C) Flow cytometry analysis of macrophages isolated from SCAT and GAT of CORT-treated WT and AdipoGR-KO mice (n=6/group). (A) Percentages of F4/80+/CD11b+ macrophages in SCAT (left panel) and GAT (right panel). (B-C) Percentage of M1-like and M2-like macrophages (with CD11c/CD206 markers) (B) and of M1-like and M2-like macrophages (with NOS2/CD206 markers) (C) in gated population from F4/80+/CD11b+ macrophages in SCAT (left panel) and GAT (right panel) of WT and AdipoGR-KO mice. Data represent the mean  $\pm$  SEM; \* P < 0.05; \*\* P < 0.01, for AdipoGR-KO versus WT mice.

190x275mm (150 x 150 DPI)

Figure 4

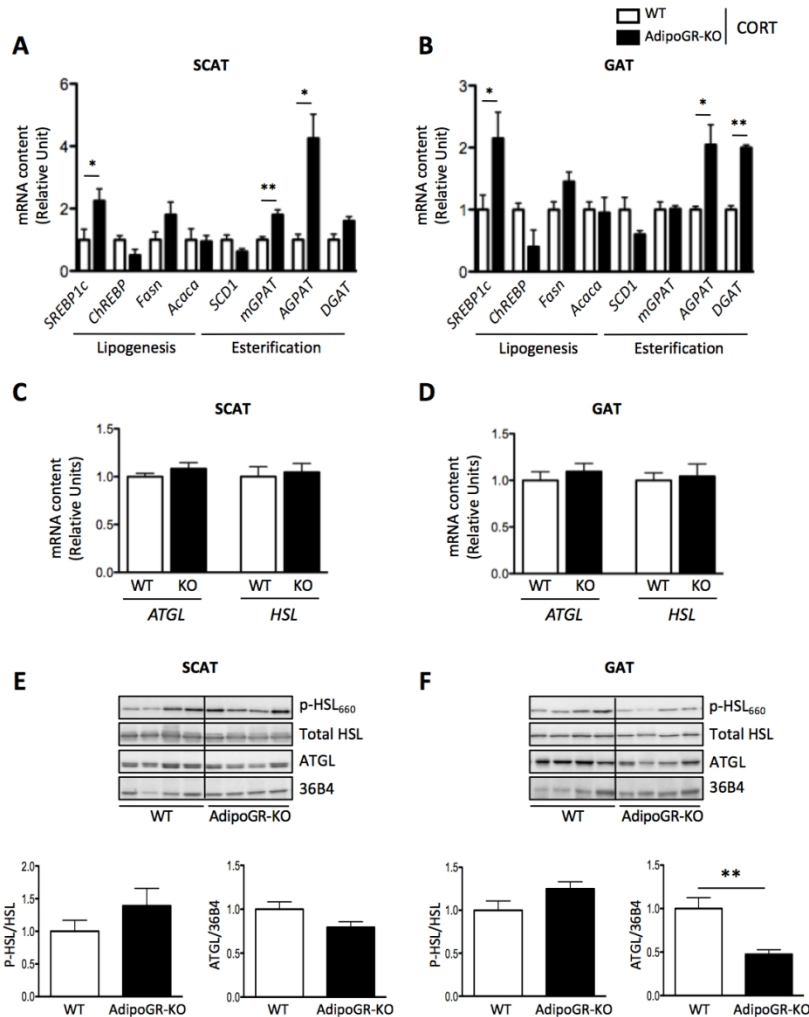


Figure 4: Adipocyte GR deficiency alters lipid metabolism enzymes content in adipose tissues of CORT-treated mice. Gene expression and protein content analysis were performed on 18-week-old mice treated with CORT for 4-weeks (n=6/group). (A-B) Relative gene expression of key enzymes of lipogenic and esterification pathways was determined by RT-qPCR in subcutaneous (SCAT) (A) and gonadal (GAT) (B) adipose tissues of refed AdipoGR-KO and WT mice (n=6/group). (C-D) Relative gene expression of key enzymes of lipolysis, ATGL and HSL, determined by RT-qPCR in total SCAT and GAT of fasted AdipoGR-KO and WT mice (n=6/group). (E-F) A representative Western Blot (upper panel) and quantification (lower panel) of key enzymes of lipolysis: ATGL and phosphorylated HSL/total HSL ratio in SCAT (E) and GAT (F) of overnight fasted AdipoGR-KO and WT mice. The 36B4 protein was used as loading control. Data represent the mean +/- SEM; \* P < 0.05; \*\* P < 0.01, for AdipoGR-KO versus WT mice.

190x275mm (150 x 150 DPI)

Figure 5

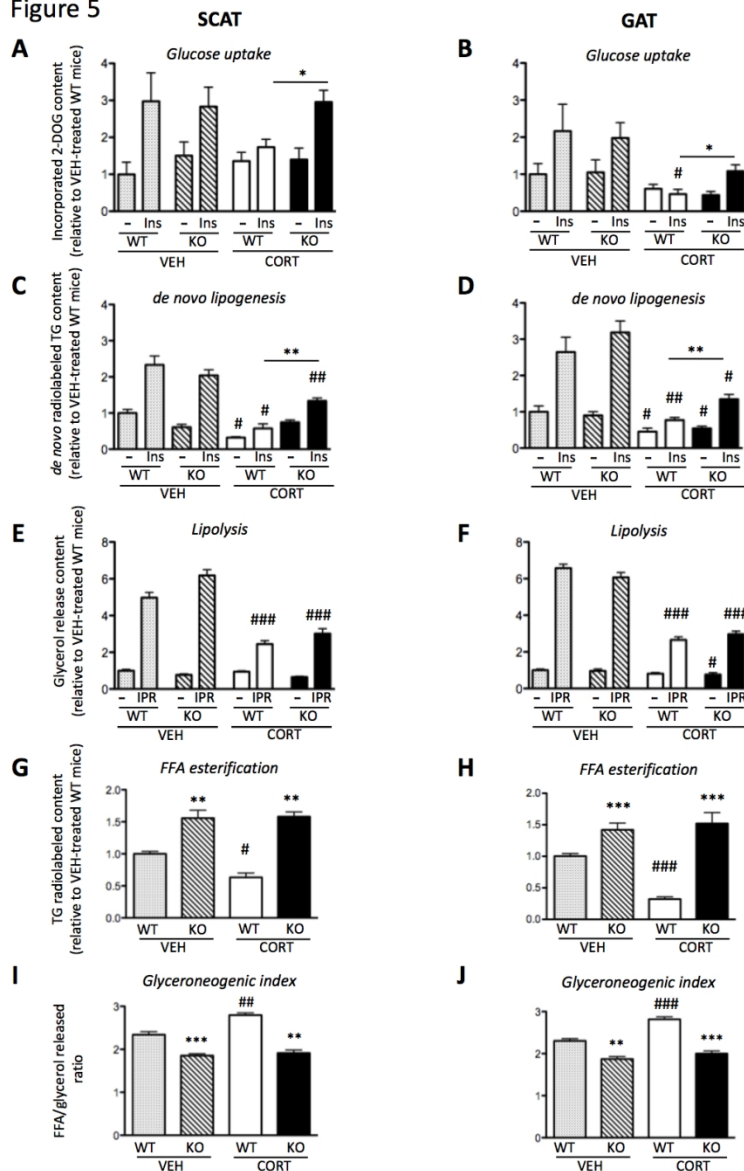


Figure 5: Metabolic responses of adipose tissue explants from AdipoGR-KO and WT mice. Eighteen-week-old mice were sacrificed after a 4-week exposure to VEH or CORT. Subcutaneous (A, C, E, G, I) and gonadal (B, D, F, H, J) fat pad explants were isolated and then tested for different metabolic activities as described in Materials and Methods (n=3-6/group). (A-B) Radiolabeled-2-deoxyglucose incorporation was performed in the presence or the absence of insulin (Ins, 100 nM) (n=6/group). (C-D) De novo lipogenic flux was performed in the presence or the absence of insulin (Ins, 100 nM) by using radiolabeled [14C]-glucose. Radiolabeled lipids were extracted and counted. (E-F) Lipolytic activity was tested in the absence or the presence of isoproterenol (IPR, 1  $\mu$ M). Glycerol released into the media was measured. (G-H) Radiolabeled pyruvate incorporation evaluates the amount of free-fatty acids (FFA) esterified and incorporated into triglycerides (TG) during a 1-h lipolytic period. Glucose transport, lipogenesis, lipolysis and reesterification activities were expressed as nmol/mg of AT/h and then arbitrary normalized to 1 from VEH-treated WT mice. (I-J) Glyceroneogenic index measured ratio of FFA versus glycerol released in the culture media. FFA/glycerol values correspond to the means of the ratios determined in each animal. Data represent the mean  $\pm$  SEM; \* P < 0.05; \*\* P < 0.01; \*\*\* P < 0.001, for AdipoGR-KO versus WT mice; # P < 0.05; ## P

<0.01; ### P <0.001, for CORT versus VEH treatment.

190x275mm (150 x 150 DPI)

Figure 6

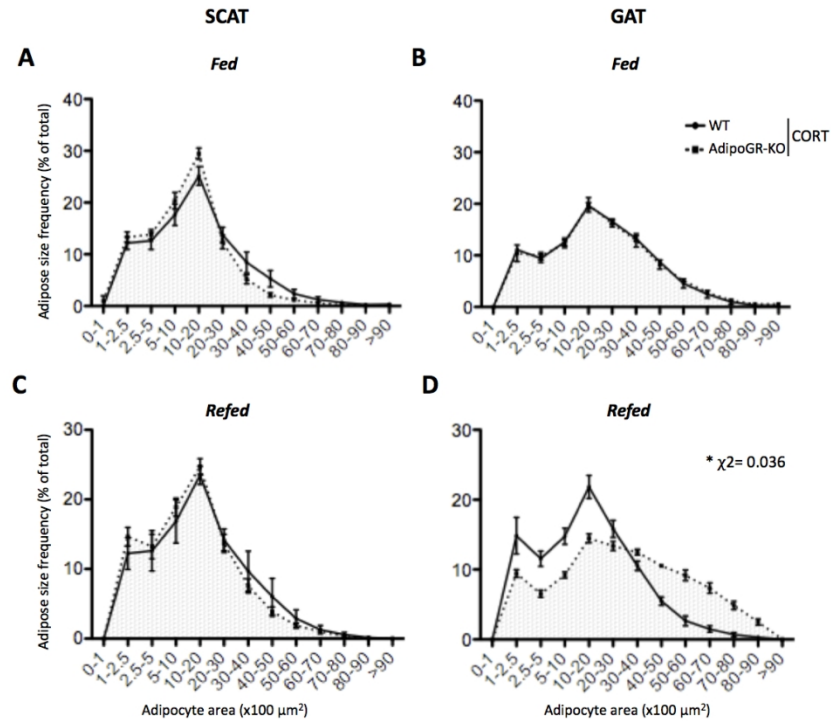


Figure 6: Adipocyte GR deficiency leads to adipocyte hypertrophy in gonadal adipose tissue of CORT-treated mice. Eighteen-week-old mice were sacrificed after a 4-week CORT exposure under fed and refeed conditions ( $n=3-4/\text{group}$ ). SCAT (A, C) and GAT (B, D) fat pads from CORT-AdipoGR-KO and WT mice were isolated for histomorphological analysis as described in Materials and Methods. Distribution of cell surfaces was determined in AT of AdipoGR-KO and WT mice under fed (A, B) and refeed (C, D) conditions.  $\chi^2$  analysis was carried out for statistical differences in adipocyte surface distribution between AdipoGR-KO and WT mice.

190x275mm (150 x 150 DPI)

Figure 7

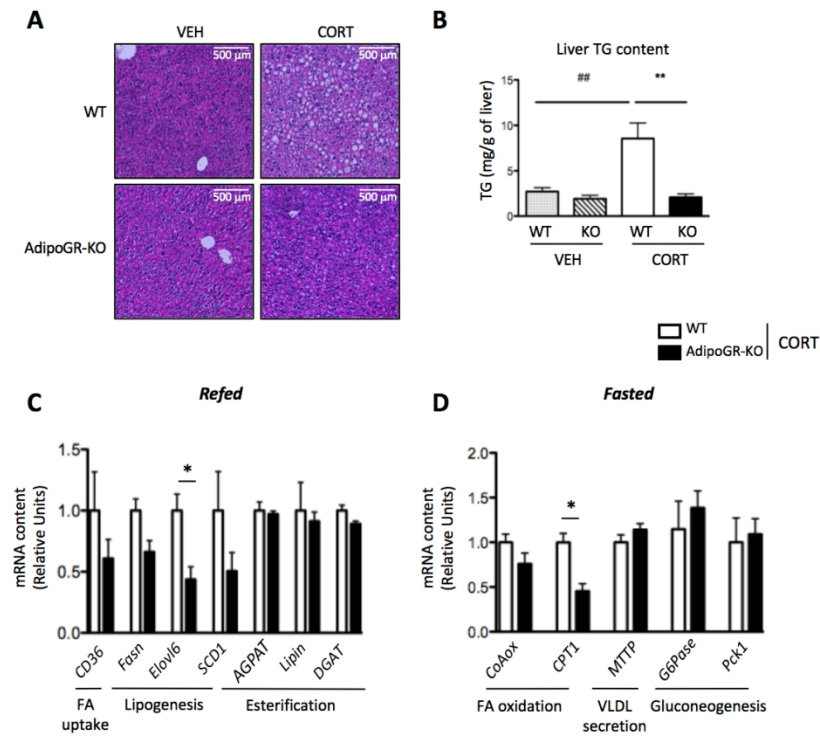


Figure 7: Adipose specific GR invalidation prevents CORT-induced-hepatic steatosis. Eighteen-week-old mice were sacrificed after a 4-week exposure to VEH or CORT under refed and fasted conditions (n=6/group). (A) Hematoxylin/eosin staining of liver sections from WT and AdipoGR-KO mice and (B) liver TG content. (C-D) Relative mRNA content of key enzymes of lipid and glucose metabolism as determined by RT-qPCR in liver of refed- (C) and fasted- (D) AdipoGR-KO and WT mice. Data represent the mean  $\pm$  SEM. \*  $P < 0.05$ ; \*\*  $P < 0.01$ , for AdipoGR-KO versus WT mice; ##  $P < 0.01$ , for CORT versus VEH treatment.

190x275mm (150 x 150 DPI)

## **Online-Only supplemental material**

### **Supporting Information:**

#### **Nutritional challenges, body mass composition and indirect calorimetry measurements**

All animals were housed with a 12 hours /12 hours light/dark cycle (8am-8pm) and had free access to water and standard chow diet (LASQCDiet® Rod16-R, LASvendi, Soest, Germany). For nutritional challenges, mice were sacrificed either after 24-hour-fasting, or refeeding (fasted for 24 h and then fed on a chow diet for 18 h), or under fed conditions. Different organs and tissues were dissected, rapidly frozen in liquid nitrogen, and kept at -80 °C.

Body mass composition was analyzed using an EchoMRI 100 Whole Body Composition Analyzer (EchoMRI, Houston, TX) according to the manufacturer's instructions (1). For measurement of food intake, spontaneous locomotor activity, energy expenditure, respiratory exchange ratio (RER) and fatty acid (FA) oxidation, each mouse was placed for 96 h in a LabMaster indirect calorimetry system after a 48-h acclimatization (TSE Systems GmbH, Bad Homburg, Germany) as described by Joly-Amado *et al* (2). FA oxidation was calculated from the following equation: fat ox (kcal/h) = energy expenditure (kcal/h) x (1-RER/0.3) according to (3). Data of calorimetric presented represent mean of at least 96 h measurement.

#### **Hormonal and biochemical analysis**

Extracted liver triglycerides (TGs) were measured with a colorimetric diagnostic kit according to the manufacturer's instructions (Triglycerides FS, DiaSys, Grabels, France). Plasma corticosterone (CORT) was measured by LC-MS as described in Fiet *et al.* (4), on samples obtained from collected blood tail vein at 8 am and 8 pm in EDTA-moistened tubes, then centrifuged at 5,000 x g for 10 min before storage at -80°C. Plasma TGs, non-esterified fatty acids (NEFAs), LDL- and HDL-

cholesterol were assayed using commercial kits (Wako Chemicals USA Inc., Richmond, VA). Plasma leptin and insulin levels were measured with the mouse immunoassay kit from R&D systems (Minneapolis, MN) and the Ultra-Sensitive Mouse Insulin ELISA Kit (Crystal Chem, Downers Grove, IL), respectively. HOMA-IR was calculated according to the formula: fasting insulin ( $\mu\text{U}/\text{mL}$ ) x fasting glucose ( $\text{mg}/\text{dL}$ ) / 405. Plasma ketone bodies were measured on whole-tail vein blood collected from fasted mice using an automatic FreeStyle Optium Neo Ketone Monitoring System (Abbott, North Chicago, IL).

### **Functional analyzes on adipose tissue explants**

Functional analyzes were carried out on subcutaneous (SCAT) and gonadal adipose tissue (GAT) explants collected from WT and AdipoGR-KO mice either treated with VEH or CORT. Glucose uptake was adapted from (5, 6). Briefly, minced SCAT and GAT explants were incubated in KRH buffer containing 2 % free fatty acid-bovine albumin serum (FFA-BSA) in the presence or the absence of insulin (100 nM) for 45 min at 37 °C, before the addition of 0.25 mM of 2-deoxyglucose and 2  $\mu\text{Ci}/\text{mL}$  [ $1\text{-}^{14}\text{C}$ ]-2-deoxy-D-glucose (Perkin Elmer, Waltham, MA) for 15 min at 37 °C. After PBS washes, explants were lysed in 500  $\mu\text{L}$  NaOH (1 M) and pH neutrality was restored by adding 500  $\mu\text{L}$  HCl (1 M). The amount of 2-deoxyglucose internalized in cells was calculated as the difference between the total amount of [ $1\text{-}^{14}\text{C}$ ]-2-deoxyglucose and the amount of non-phosphorylated [ $1\text{-}^{14}\text{C}$ ]-2-deoxyglucose found in supernatants.

Lipogenic activity, FFA re-esterification and lipolysis were adapted from (7). Lipogenic activity was determined on explants incubated in Krebs-Ringer bicarbonate (KRB) buffer containing 3% FFA-BSA with [ $^{14}\text{C}$ ]-glucose (2  $\mu\text{Ci}/\text{mL}$ ), 1 mM glucose in the presence or the absence of 100 nM insulin. Two hours later, adipose tissue (AT) explants were frozen in liquid nitrogen before lipid

extraction using a simplified method of Bligh and Dyer (8). Radiolabeled TGs incorporated into the cells were determined by scintillation counting.

For FFA re-esterification, AT explants were incubated in KRB buffer containing 3 % FFA-BSA, [<sup>14</sup>C-1]-pyruvate (2 μCi/mL), 0.5 mM pyruvate, and 1 μM isoproterenol. Lipolytic FFA and glycerol released into the media were measured after 1 hour incubation. Tissue explants were then frozen in liquid nitrogen before lipid extraction using a simplified method of Bligh and Dyer (8). The [<sup>14</sup>C-1] pyruvate incorporated into the TGs was counted and was used to appreciate the level of FFA re-esterified during the lipolytic process.

Basal and stimulated lipolysis were determined on tissue explants incubated in KRB buffer containing 3% FFA-BSA with or without 1 μM isoproterenol under constant agitation. Glycerol and FFA released into the media was determined using commercial kits (Wako Chemicals USA Inc., Richmond, VA).

### **Isolation of adipocyte fraction**

SCAT and GAT collected from WT and AdipoGR-KO mice were digested in a solution containing collagenase A (1 mg/mL) (Roche, Basel, Switzerland) in PBS with 2 % bovine serum albumin (BSA) (Eurobio, Les Ulis, France) and under agitation for 1 hour at 37°C. The mixture was then poured through a 150 μm nylon filter and the floating adipocytes were separated from the stromal vascular fraction (SVF) following series of washes with Dulbecco's Modified Eagle Medium as described previously (27). Adipocyte supernatants were collected for RNA extraction in 750 μL of Qiazol Lysis Reagent (QIAGEN, Venlo, Netherlands) and maintained at -20°C until RNA extraction and gene expression analysis by real-time PCR. Adipocyte fraction was also collected

for protein content analysis. The floating adipocyte fraction was thus removed and stored at  $-80^{\circ}\text{C}$  until use.

### **RNA extraction and RT-qPCR analysis**

Total RNA from tissues and adipocyte fractions were isolated by Qiazol extraction and purification using Qiagen RNeasy minicolumns according to the manufacturer's instructions (Qiagen, Courtaboeuf, France). For real-time RT-qPCR analysis, 500 ng of total RNA was reverse-transcribed using the High Capacity cDNA Reverse Transcription kit (Applied Biosystems, Foster City, CA). cDNA was amplified using specific primers and the SYBR Green PCR Master mix (Applied Biosystems, Foster City, CA) according to the manufacturer's instructions. Reactions were performed using a Light Cycler system (Roche Diagnostics, Meylan, France). Relative gene expression was determined as arbitrary unit as the ratio of target transcripts to the reference genes, 36B4 and HPRT. Primers sequences are available upon request.

### **Adipose fraction protein Analysis**

Mouse tissues and adipocyte fractions were lysed as described in (9). Equal protein amounts (20  $\mu\text{g}$ ) were separated by SDS-PAGE, transferred to nitrocellulose membrane and immunodetected with antibodies listed in supplemental Table 1. Autoradiograms were quantified using an imageJ program (Chemi Genius2 scan, GeneSnap; Syngene, Cambridge, UK).

### **References**

1. Taicher GZ, Tinsley FC, Reiderman A, Heiman ML. Quantitative magnetic resonance (QMR) method for bone and whole-body-composition analysis. *Anal Bioanal Chem* 2003;377: 990-1002

2. Joly-Amado A, Denis RG, Castel J, Lacombe A, Cansell C, Rouch C, Kassis N, Dairou J, Cani PD, Ventura-Clapier R, Prola A, Flamment M, Fougelle F, Magnan C, Luquet S. Hypothalamic AgRP-neurons control peripheral substrate utilization and nutrient partitioning. *EMBO J.* 2012;31: 4276-4288
3. Bruss MD, Khambatta CF, Ruby MA, Aggarwal I, Hellerstein MK. Calorie restriction increases fatty acid synthesis and whole body fat oxidation rates. *Am J Physiol Endocrinol Metab* 2010;298: E108-116
4. Fiet J, Le Bouc Y, Guéchet J, Hélin N, Maubert M-A, Farabos D, Lamazière A. A Liquid Chromatography/Tandem Mass Spectrometry Profile of 16 Serum Steroids, Including 21-Deoxycortisol and 21-Deoxycorticosterone, for Management of Congenital Adrenal Hyperplasia *J Endocr Soc* 2017;1: 186-201
5. Rogers PM, Mashtalir N, Rathod MA, Dubuisson O, Wang Z, Dasuri K, Babin S, Gupta A, Markward N, Cefalu WT, Dhurandhar NV. Metabolically favorable remodeling of human adipose tissue by human adenovirus type 36. *Diabetes* 2008;57: 2321-2331
6. Attané C, Daviaud. D., Dray C, Dusaulcy R, Masseboeuf M, Prévot D, Carpéné C, Castan-Laurell I, Valet P. Apelin stimulates glucose uptake but not lipolysis in human adipose tissue ex vivo. *J Mol Endocrinol* 2011;46: 21-28
7. Tordjman J, Chauvet G, Quette J, Beale EG, Forest C, Antoine B. Thiazolidinediones block fatty acid release by inducing glyceroneogenesis in fat cells. *Tordjman J1, Chauvet G, Quette J, Beale EG, Forest C, Antoine B. J Biol Chem* 2003;278: 18785-18790
8. Bligh EG, Dyer WJ. A rapid method of total lipid extraction and purification. *Can J Biochem Physiol.* 1959;37: 911-917
9. Dubuquoy C, Robichon C, Lasnier F, Langlois C, Dugail I, Fougelle F, Girard J, Burnol AF, Postic C, Moldes M. Distinct regulation of adiponutrin/PNPLA3 gene expression by the transcription factors ChREBP and SREBP1c in mouse and human hepatocytes. *J Hepatol.* 2011;55: 145-153

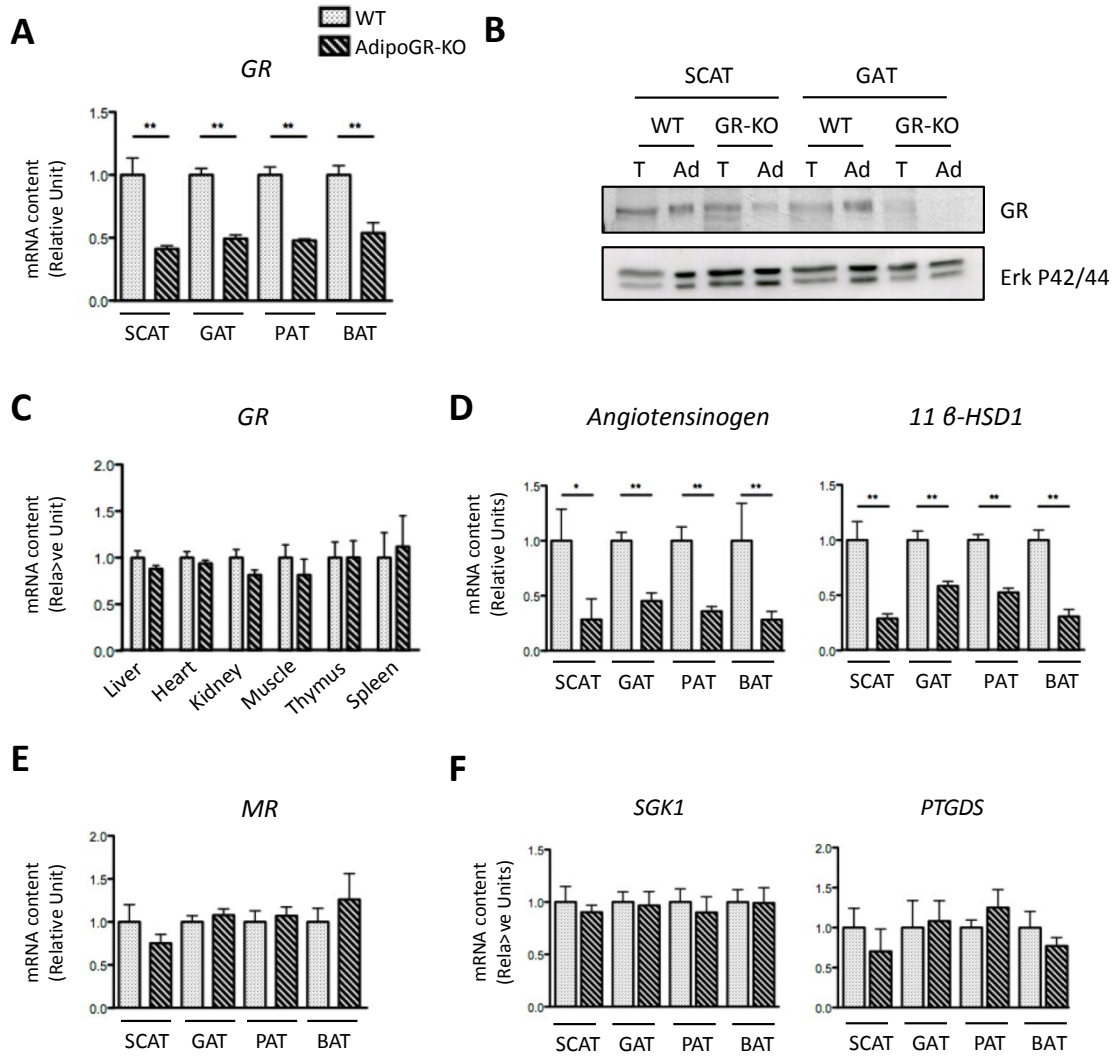
**Supplemental Table 1: Antibodies**

Antibodies	Company	dilution
Adiponectin	# PA1-054 ; Thermo Fisher Scientific (Waltham, MA)	1 :500
ATGL	# 2138 ; Cell Signaling Technology (Danvers, MA)	1 :1000
GR	# 12041 ; Cell Signaling Technology (Danvers, MA)	1 :1000
Phosphorylated P-Akt (P-Ser 473)	# sc-7985-R ; Santa Cruz Biotechnology (Dallas, TX)	1 :1000
Total Akt	# 9272S ; Cell Signaling Technology (Danvers, MA)	1 :1000
Phosphorylated P-HSL (P-Ser 660)	# 4126; Cell Signaling Technology (Danvers, MA)	1 :1000
Total HSL	# 4107 ; Cell Signaling Technology (Danvers, MA)	1 :1000
Total Erk	# 9102S ; Cell Signaling Technology (Danvers, MA)	1 :1000
36B4	# ab88872; Abcam (Cambridge, UK)	1 :500
Anti-mouse	# 7076S ; Cell Signaling Technology (Danvers, MA)	1 :10 000
Anti-rabbit	# 7074S ; Cell Signaling Technology (Danvers, MA)	1 :10 000

## Supplemental figures

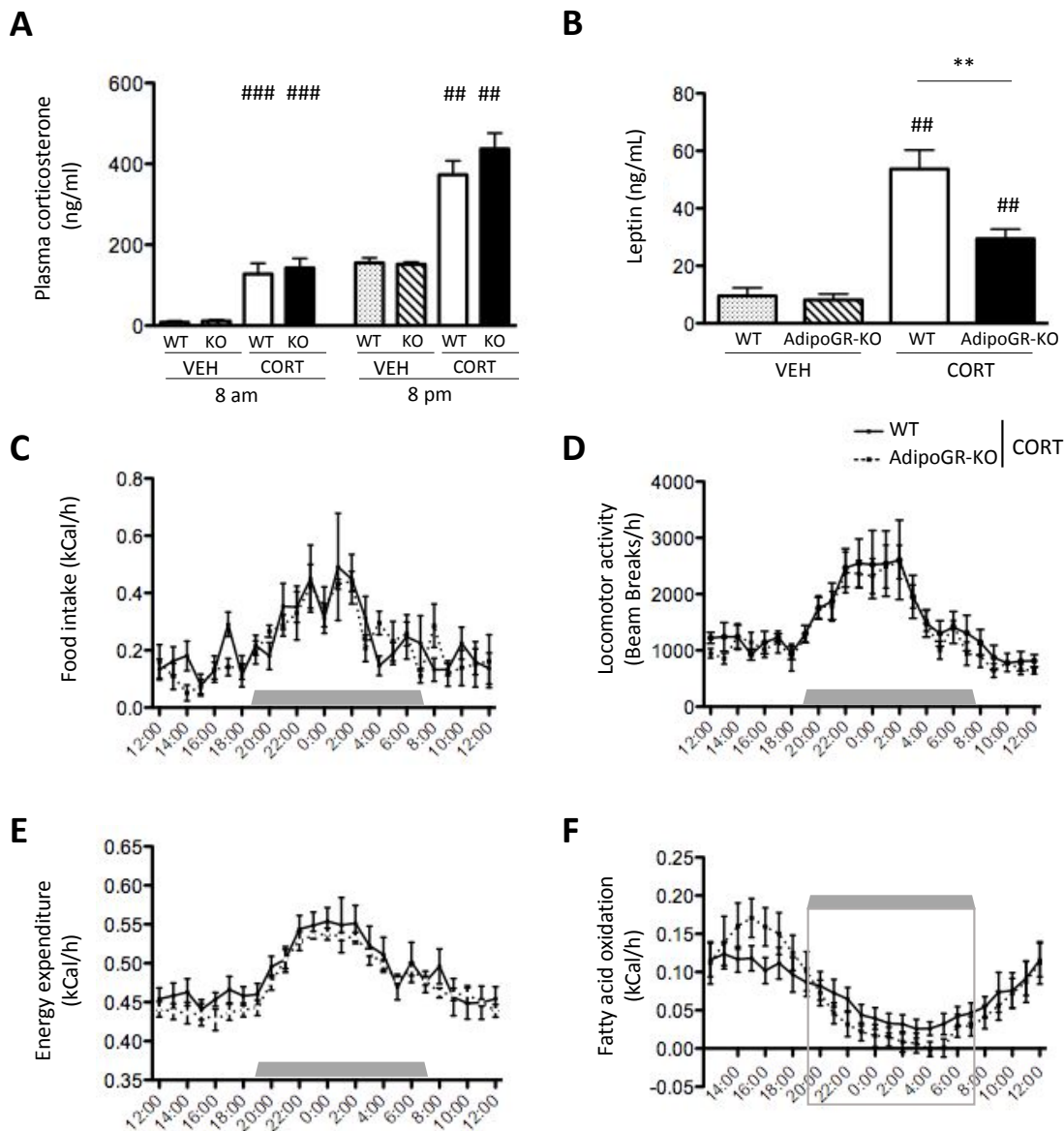
### Supplemental figure S1: Validation of the AdipoGR-KO mouse model

Eighteen-week-old WT and AdipoGR-KO mice were sacrificed on a fed state (n=6/group). **(A)** Relative *GR* gene expression was determined by RT-qPCR in total subcutaneous (SCAT), gonadal (GAT), perirenal (PAT) and brown adipose tissue (BAT) of mice. **(B)** A representative Western Blot of GR protein content in total (T) and adipocyte fraction (Ad) of SCAT and GAT of AdipoGR-KO and WT mice. The Erk P42/44 protein was used as a loading control. **(C)** Relative *GR* gene expression was determined by RT-qPCR in non-adipose tissues of AdipoGR-KO and WT mice. **(D)** Relative mRNA content of GR target genes: *angiotensinogen* and *11 $\beta$ -HSD1* in SCAT, GAT, PAT and BAT of AdipoGR-KO and WT mice. **(E-F)** Relative mRNA content of MR **(E)** and its target genes **(F)**: *SGK1* and *PTGDS* in SCAT, GAT, PAT and BAT of AdipoGR-KO and WT mice. Data are presented as the mean +/- SEM; \*  $P < 0.05$ ; \*\*  $P < 0.01$ , for AdipoGR-KO *versus* WT mice.



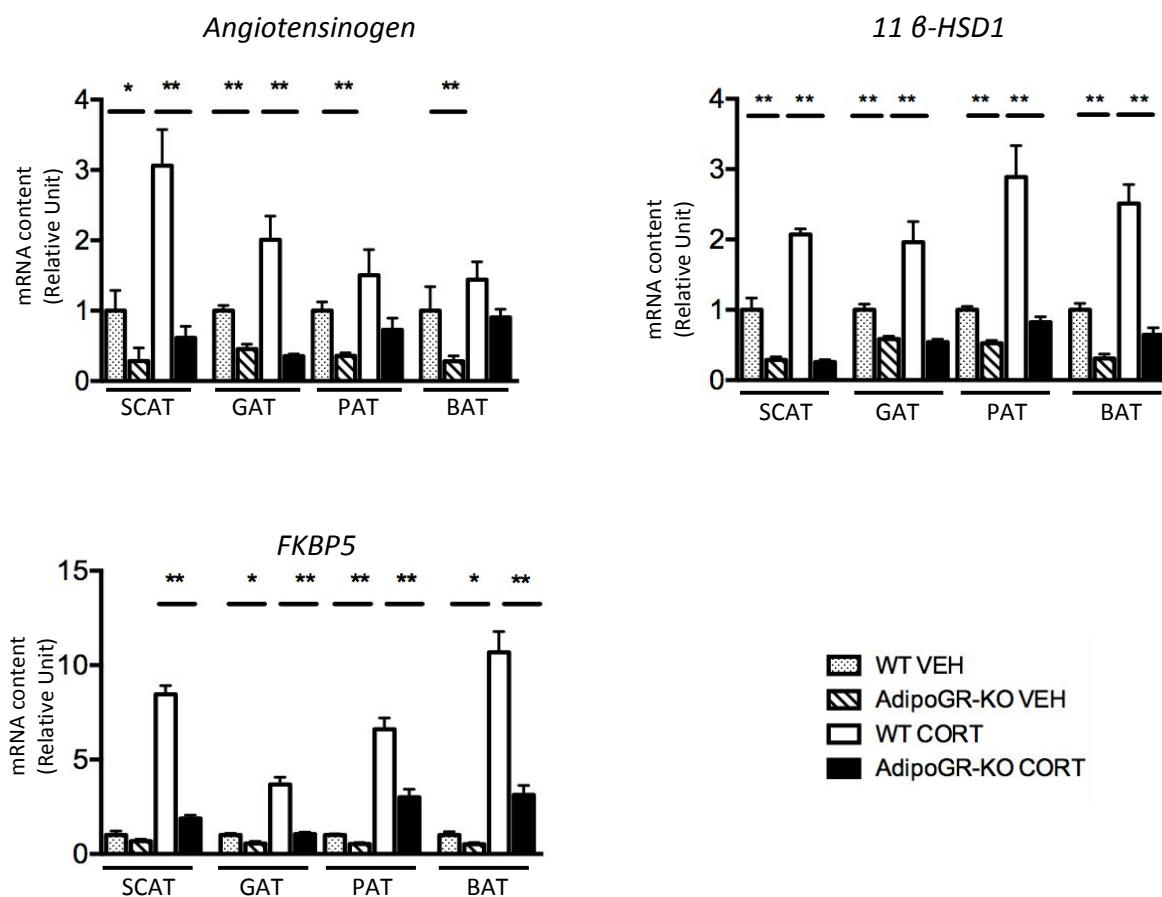
### Supplemental figure S2: Hormonal and energetic parameters of WT and AdipoGR-KO mice

Corticosterone (8am and 8pm) (A) and leptin (B) levels were measured in the plasma of VEH or CORT-treated mice (n=6/group). (C-F) Food intake (C), locomotor activity (D), energy expenditure (E), and fatty acid oxidation (F) were measured in CORT-treated WT- and AdipoGR-KO mice as described in *Supplemental Materials and Methods* (n=6/group). Data are presented as the mean  $\pm$  SEM; \*\*  $P < 0.01$ , for AdipoGR-KO versus WT mice; ##  $P < 0.01$ ; ####  $P < 0.001$ , for CORT- versus VEH-treated WT mice.



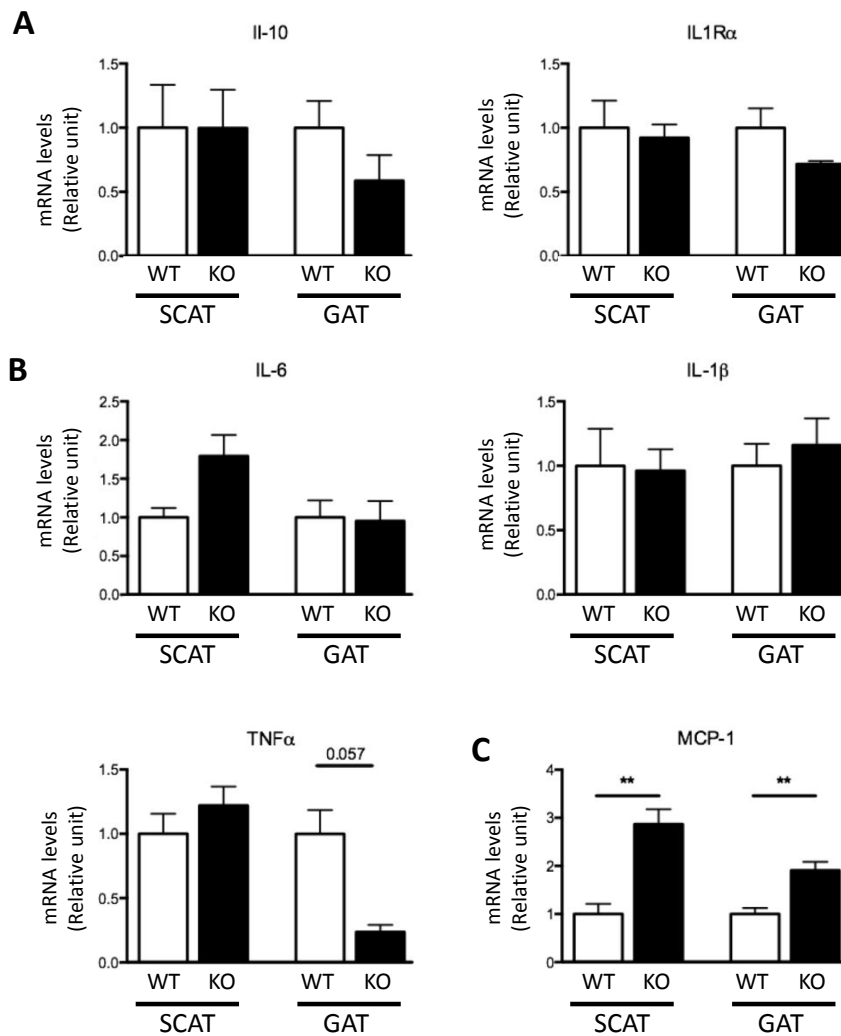
### Supplemental figure S3: Expression of GR target genes in adipose tissues of WT and AdipoGR-KO mice

Eighteen-week-old mice were sacrificed after a 4-week exposure to vehicle (VEH) or corticosterone (CORT) (n=6/group). Relative mRNA content of GR target genes: *angiotensinogen*, *11 $\beta$ -HSD1* and *FKBP5* in SCAT, GAT, PAT and BAT of AdipoGR-KO and WT mice. Data are presented as the mean  $\pm$  SEM; \*  $P < 0.05$ ; \*\*  $P < 0.01$ , for AdipoGR-KO versus WT mice.



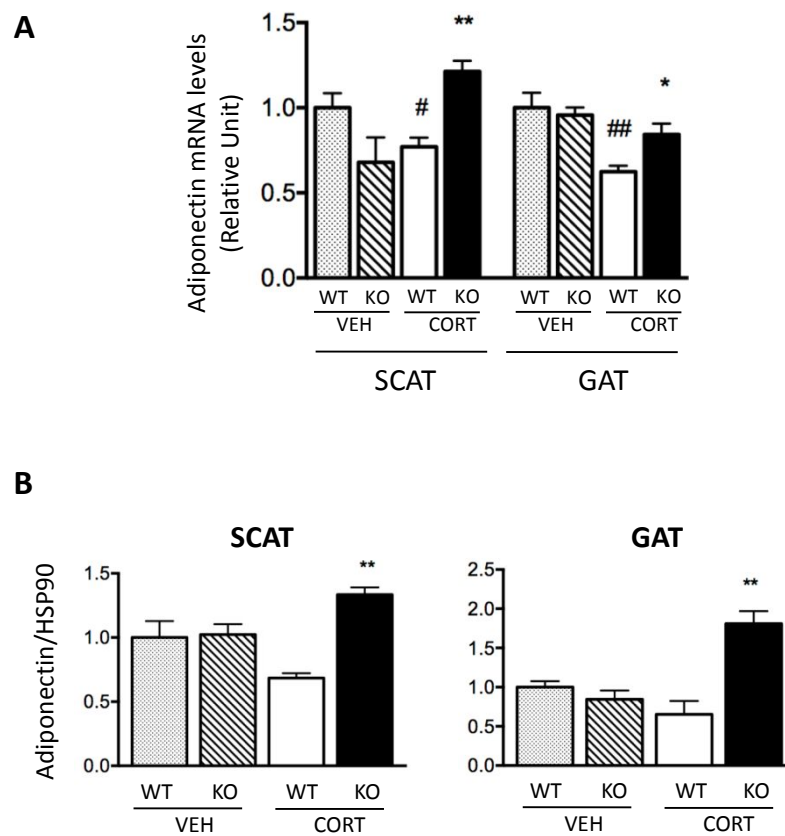
### Supplemental figure S4: Cytokine and chemokine gene expression in SCAT and GAT of WT and AdipoGR-KO mice

Eighteen-week-old mice were sacrificed after a 4-week exposure to corticosterone (CORT) (n=6/group). Adipocytes were isolated from subcutaneous (SCAT), and gonadal (GAT) adipose tissues of re-fed-AdipoGR-KO and WT mice. Relative mRNA content of anti-inflammatory (IL-10, IL-1Ra) (**A**) and pro-inflammatory (IL-6, IL-1 $\beta$ , TNF $\alpha$ ) (**B**) cytokines in adipocyte fractions of SCAT and GAT of AdipoGR-KO and WT mice. (**C**) Relative mRNA content of the MCP-1 chemokine in adipocyte fractions of SCAT and GAT from AdipoGR-KO and WT mice (n=6/group). Data are presented as the mean  $\pm$  SEM. \*\*  $P < 0.01$ , for AdipoGR-KO *versus* WT mice.



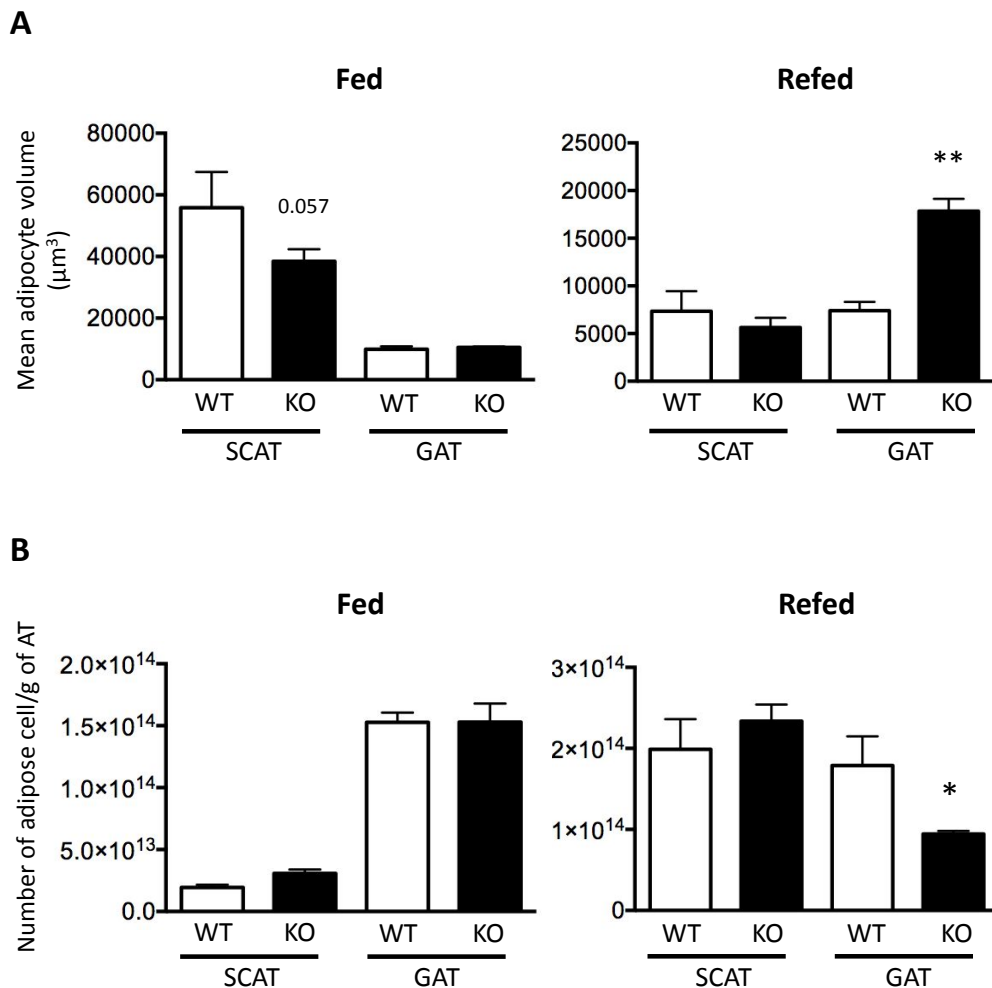
### Supplemental figure S5: Adiponectin mRNA and protein content in SCAT and GAT of WT and AdipoGR-KO mice

Gene expression and protein content analysis were performed on 18-week-old mice treated with VEH- or CORT for 4-weeks (n=6/group). **(A)** Relative gene expression of adiponectin determined by RT-qPCR in total subcutaneous adipose tissue (SCAT) and gonadal adipose tissue (GAT) of AdipoGR-KO and WT mice (n=6/group). **(B)** Quantification of Western Blot of the ratio adiponectin/HSP90 in SCAT and GAT of AdipoGR-KO and WT mice. The HSP90 protein was used as loading control. Data represent the mean  $\pm$  SEM; \*  $P < 0.05$ ; \*\*  $P < 0.01$ , for AdipoGR-KO versus WT mice. #  $P < 0.05$ ; ##  $P < 0.01$ , for CORT versus VEH treatment.



### Supplemental figure S6: Adipocyte volume and number in SCAT and GAT of WT and AdipoGR-KO mice

Eighteen-week-old mice were sacrificed after a 4-week CORT exposure (n=3-4/group). Subcutaneous (SCAT) and gonadal (GAT) fat pads from CORT-AdipoGR-KO and WT mice were isolated for histomorphological analysis as described in *Materials and Methods*. **(A)** The mean adipocyte volume was determined from the distribution of cell surfaces in adipose tissues of AdipoGR-KO and WT mice under fed (**left panel**) and refed (**right panel**) conditions. **(B)** The number of adipose cells were determined per gram of SCAT and GAT of AdipoGR-KO and WT mice under fed (**left panel**) and refed (**right panel**) conditions. Data represent the mean  $\pm$  SEM; \*  $P < 0.05$ ; \*\*  $P < 0.01$ , for AdipoGR-KO *versus* WT mice.



### Supplemental figure S7: Gene expression of key adipogenic transcription factors in SCAT and GAT of WT and AdipoGR-KO mice

Eighteen-week-old mice were sacrificed after a 4-week exposure to corticosterone (CORT) (n=6/group). Gene expression of the transcription factors *CEBP $\beta$* , *CEBP $\delta$* , *CEBP $\alpha$*  and *PPAR $\gamma$*  was determined by RT-qPCR in subcutaneous (SCAT), and gonadal (GAT) adipose tissues of re-fed-AdipoGR-KO and WT mice. Data are presented as the mean  $\pm$  SEM.

